

Tailored Forecasting from Short Time Series via Meta-learning

Declan A. Norton,^{1, a)} Edward Ott,^{1, 2, 3} Andrew Pomerance,⁴ Brian Hunt,^{5, 6} and Michelle Girvan^{1, 2, 5, 7}

¹⁾*Department of Physics, University of Maryland, College Park, MD 20742 USA*

²⁾*Institute for Research in Electronics and Applied Physics, University of Maryland, College Park, MD 20742 USA*

³⁾*Department of Electrical and Computer Engineering, University of Maryland, MD 20742 USA*

⁴⁾*Potomac Research LLC, Alexandria, VA 22314 USA*

⁵⁾*Institute for Physical Science and Technology, University of Maryland, College Park, MD 20742 USA*

⁶⁾*Department of Mathematics, University of Maryland, College Park, MD 20742 USA*

⁷⁾*Santa Fe Institute, Santa Fe, NM 87501 USA*

(Dated: 28 January 2025)

Machine learning (ML) models can be effective for forecasting the dynamics of unknown systems from time-series data, but they often require large amounts of data and struggle to generalize across systems with varying dynamics. Combined, these issues make forecasting from short time series particularly challenging. To address this problem, we introduce Meta-learning for Tailored Forecasting from Related Time Series (METAFORS), which uses related systems with longer time-series data to supplement limited data from the system of interest. By leveraging a library of models trained on related systems, METAFORS builds tailored models to forecast system evolution with limited data. Using a reservoir computing implementation and testing on simulated chaotic systems, we demonstrate METAFORS' ability to predict both short-term dynamics and long-term statistics, even when test and related systems exhibit significantly different behaviors and the available data are scarce, highlighting its robustness and versatility in data-limited scenarios.

I. INTRODUCTION

Accurate forecasting of dynamical systems is of practical importance across diverse domains¹ including weather and climate science², neuroscience^{3,4}, epidemiology⁵, and finance⁶. For many dynamical systems, however, we lack a sufficient knowledge-based model (i.e., mathematical or physical) to provide useful predictions. Data-driven approaches to infer a model of a system from its past evolution are highly valuable in these cases^{7,8}. While powerful, these machine learning (ML) forecasters are typically data-intensive and brittle^{9,10}: they require lengthy training series and become inaccurate if the dynamics of the system to be predicted, i.e. the test system, differ even slightly from those seen in training. They thus struggle in many consequential scenarios. For example, public health officials responding to the initial outbreak of a virus may find that early data are insufficient to train an ML model for the spread of infection, and that one trained on data from another jurisdiction or previous outbreak does not generalize well. The motivation of this work is to facilitate useful forecasting when only a short time series is available from the system of interest. We focus on situations where no helpful knowledge-based model is available, but anticipate that our approach could also apply to hybrid architectures that integrate knowledge-based models with ML components^{2,11}.

The method we introduce amalgamates learned knowledge from ML forecasters trained on related, data-rich processes to improve performance on similarly related processes for which data are limited. As such, our work builds on prior studies in multi-task learning and meta-learning. These frameworks aim to reduce the data-intensity and brittleness of ML models by leveraging knowledge from tasks related to the one at hand.

Multi-task learning algorithms address data scarcity by training a single ML model on the union of all data from a set of training systems. No emphasis is placed on any particular training system or on the test system – the goal is to improve performance generically^{12,13}. In the context of time series forecasting, a multi-task learning approach would train a single model on a collection of time series from systems which each exhibit different dynamics. Multi-task learning may make the model less brittle to discrepancies between the dynamics of the training and test systems, but the training data that are most relevant to the behavior of the test system are often diluted with considerably less relevant data¹². Thus, models trained by multi-task learning techniques may not achieve the desired performance for individual tasks.

Meta-learning, by contrast, assumes that sufficient data are available to train models for individual tasks. The goal of meta-learning, or ‘learning about learning’ is to generalize knowledge from these individual tasks to quickly adapt to new, unseen tasks. This process leverages prior learning to improve learning efficiency and performance specifically on individual future tasks^{14–17}. Meta-learning has been used for a variety of purposes^{14–16}: hyperparameter optimization¹⁸, algorithm selection and combination^{19,20}, and few- or zero-shot learning. We are concerned mostly with this final goal – to tailor the trainable parameters of a model to a test system, given only a few data points from that system.

In this work, we construct a meta-learning approach for time series prediction that draws on a library of ML models with memory. By “memory” we mean that the output of the ML model depends not only on measurements of the current state of the system being forecasted, but also on measurements at previous times. This is the case for both ML architectures with intrinsic memory – eg. those based on recurrent neural networks, including long short-term memory models (LSTMs), gated recurrent units (GRUs), and reservoir

^{a)}Correspondence email address: nortonde@umd.edu

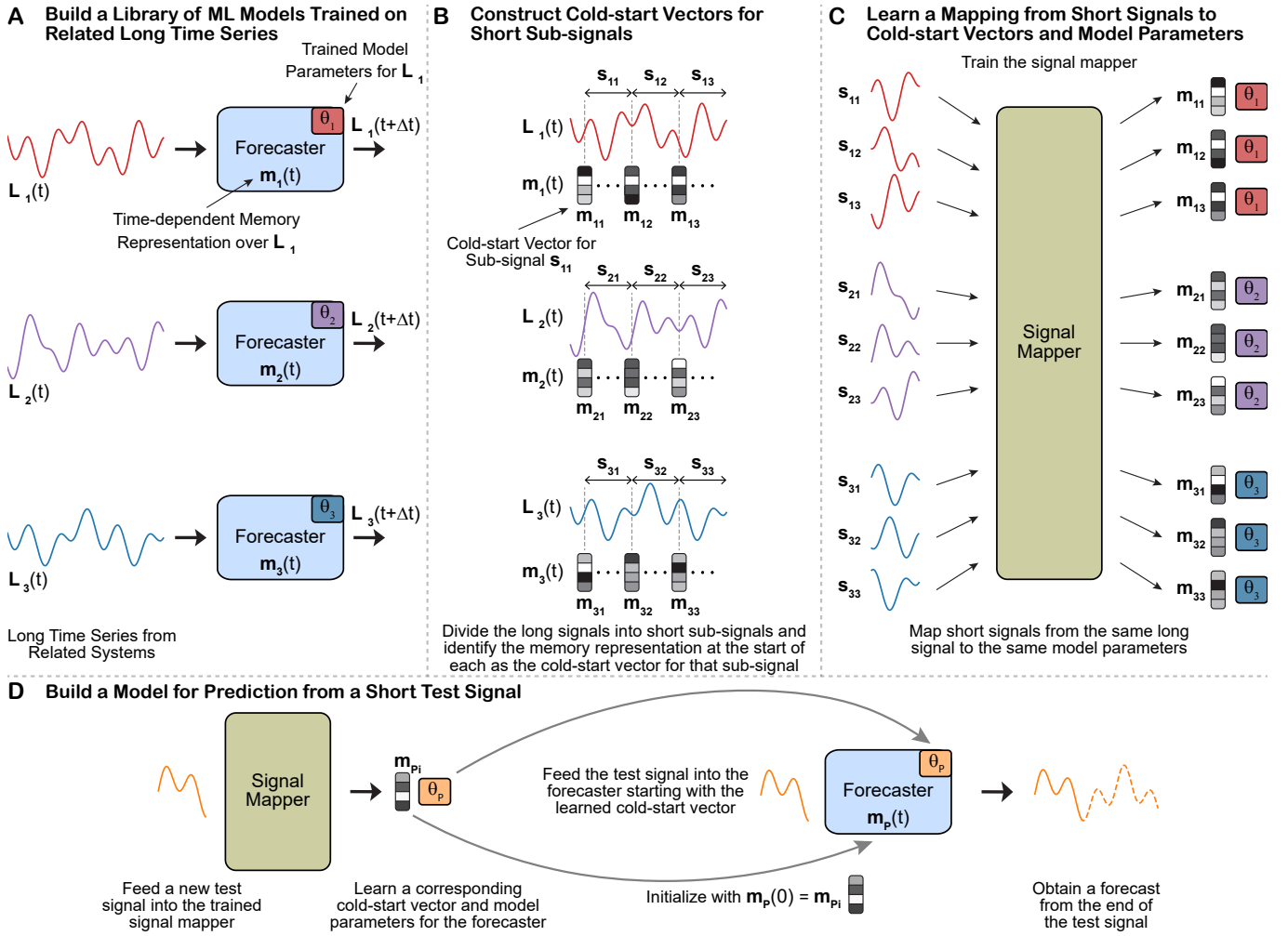


FIG. 1: **A Schematic of the METAFORS Meta-learning Method**

(A) We train the forecaster separately on each of the available long training series, L_i , to construct both a model representation of each corresponding dynamical system, and a cold-start vector at every time-step. (B) We then divide the long signals into short sub-signals, s_{ij} , that are the same length as the available test signals and (C) train the signal mapper to map these short signals to cold-start vectors, m_{ij} , corresponding to their start times, and appropriate model parameters, θ_i , for the forecaster, as in Sections IV B 2 to IV B 4. (D) Given a test signal, s_{test} , the signal mapper learns a suitable cold-start vector, m_{pi} , and model parameters, θ_p . To make a prediction, we initialize the forecaster with the learned cold-start vector and drive the forecaster with the test signal to mitigate errors in the learned cold-start vector. Finally, we evolve the forecaster autonomously with the learned parameters.

computers (RCs), for which the memory is encoded in the network’s internal state – and ML architectures without intrinsic memory that explicitly include time-delayed measurements in their input – e.g., next-generation reservoir computers and certain implementations of feedforward neural networks and kernel machines. ML models with memory are especially well-suited for time series prediction because they can extract information about unmeasured variables from the dynamics of measured variables. However, when we need to make forecasts from very short test signals, the model’s memory dependence creates an additional challenge: to predict accurately, the memory must be initialized consistently with the current state of the test system^{21–25}. Often, a substantial amount of data immediately preceding the start of a forecast is required

for this purpose. In this case, if the available data are insufficient to initialize the ML model’s memory, forecasts will be either unobtainable or inaccurate, even if the model has been well-trained. In other words, memory-based ML models struggle to produce useful forecasts from a ‘cold start.’ We refer to a suitable initialization of a model’s internal state or memory as a ‘cold-start vector.’

In the scenarios we consider, the short time series data from the system of interest does not by itself provide enough information to accomplish the desired forecasting task. However, we assume that we are operating within the common situation where additional potentially relevant information is available that can be used alongside the short time series to enable accurate forecasting. Specifically, we assume that this additional

information comes in the form of prior, more extensive measurements from other systems – and/or data from model simulations – whose dynamics we suspect are "related" to those of our system of interest.

Meta-learning for Tailored Forecasting from Related Time Series (METAFORS), which we introduce here, allows memory-based ML forecasters to overcome the challenges of data-intensity, brittleness, and cold-starting. METAFORS exploits a collection of long training time series from related dynamical systems, using two levels of learning, to construct suitable models of new, similarly-related test systems for which data are limited. Two-level learning is a common feature in meta-learning approaches¹⁴.

In our first learning level, we train separate forecasting models (Fig. 1A) for each long training series $L_i(t)$. These models share the same base network architecture, and differ only in their trained model parameters, which we denote by a vector θ_i . Once trained, each model becomes a representation of its corresponding system's dynamics. We also extract multiple short signals s_{ij} from each long signal, and during the training we record the model's memory immediately prior to inputting s_{ij} as a cold-start vector m_{ij} (Fig. 1B). We store the short signals, along with their corresponding cold-start vectors and trained model parameters, in a 'library'.

In the second learning level, another ML model, which we call the 'signal mapper', draws on this library to learn a direct mapping from short observation signals to appropriate forecaster parameters and cold-start vectors (Fig. 1C). The training data consists of inputs s_{ij} and corresponding target outputs (m_{ij}, θ_i) . By leveraging this amalgamated knowledge, the signal mapper can then construct tailored forecasters for test signals with previously unseen or unknown dynamics (Fig. 1D). Importantly, METAFORS requires no explicit knowledge of the parameters or functional forms that govern the dynamics of either the library or test signals; it generalizes from the library models in an entirely data-driven manner.

Previous studies have shown that memory-based ML forecasters, when provided with explicit knowledge of either a relevant dynamical parameter^{26–29} or a contextual label³⁰ for each training and test series, can successfully forecast the long-term statistics, or climate, of test systems whose dynamics were not seen during training. These approaches are especially valuable in applications where we seek to predict a system's behavior for a particular regime of a prescribed parameter—for example, projecting how the climate may evolve as atmospheric CO₂ levels rise. By contrast, METAFORS tackles a related but distinct challenge: enabling rapid generalization to test systems where only short time series are available, and the relevant dynamical parameters remain unknown.

The meta-learning framework – that is, learning to extract information from related tasks and utilize that information for the task at hand – facilitates this generalization in the absence of explicit context indicators. Several studies have explored meta-learning algorithms for zero-shot and few-shot prediction in applications beyond forecasting^{31–35}. We are aware, however, of only a handful of works that directly address meta-learning for dynamical systems^{36–40}. Among these approaches, METAFORS is important because: it does

not rely on any specific neural network architectures; it both initializes and generalizes the forecaster model (and therefore readily accommodates forecasters with memory); it requires no awareness of dynamical parameters and little or no domain-knowledge; and it requires no re-training or optimization when presented with new test systems. METAFORS also demonstrates the versatility of meta-learning approaches to forecasting problems. It can forecast both climate and short-term evolution, generalize the forecaster to new test systems with qualitatively different behaviors, and learn to simultaneously represent dynamical systems of distinct functional forms.

The way in which METAFORS deals with ML models with memory for forecasting is appealing in part because of existing and potential connections between information processing in artificial and biological neural networks. Recent work^{41,42} has employed artificial neural network models with memory for time series forecasting to suggest biologically feasible learning paradigms that capture the flexibility of biological neural systems to learn different tasks simultaneously. However, these multi-task learning frameworks either manually separate the distributions of observed data from different tasks⁴¹ or require a context-based control-parameter⁴² to identify the task at hand. Here, we demonstrate that METAFORS can achieve the same flexibility without any explicit context-awareness and with considerable overlap in the distributions of the observed data.

To demonstrate METAFORS' utility, we employ a similar reservoir computing implementation (Section IV A) of memory-based ML forecasting models as used in the aforementioned papers that develop multi-task learning approaches for time series forecasting. Reservoir computers (RCs) have been shown to perform well for data-driven prediction and analysis of dynamical systems^{43–45}, even those whose behavior is complex (e.g., dynamics on extended networks^{46,47}) or those that exhibit sensitivity to initial conditions^{11,26,45,47–52} (i.e., "chaotic" systems). Here, for simplicity, we use RCs as both the forecaster and the signal mapper. We emphasize, however, that in typical implementations, RCs also struggle with data-intensity²³, brittleness^{10,53}, and cold-starting^{21–24}.

In Section II, we show that METAFORS enables RC forecasting models to overcome each of these challenges. First, we demonstrate that METAFORS captures the long-term statistics, i.e. climate, of unseen test systems. Trained, for example, on just a few stationary trajectories from the chaotic regime of the logistic map⁵⁴, METAFORS can replicate the map's dynamics across a large portion of its bifurcation diagram from short test signals with unknown dynamical parameters. Even when the library contains some ML models trained on logistic maps and others trained on Gauss iterated maps⁵⁵, METAFORS can construct the bifurcation diagrams of both – a difficult problem requiring it to implicitly determine the system type from a short test signal and build tailored forecasters in regions not covered in the library. In Section II E, we show that METAFORS accurately forecasts the short-term evolution and climate of chaotic Lorenz-63 systems⁵⁶ with both fully-observed and partially-observed states. We highlight that when the available test signals are

very short, the cold-start vectors learned by METAFORS are essential to accurate forecasting. Moreover, when the test and training systems are known to have the same underlying dynamics, METAFORS can be used to cold-start an RC forecaster with no more training data than is traditionally required. In Section III, we discuss the implications of our results and in Section IV we detail our implementation of RC forecasting models and the scope of METAFORS.

Finally, although we illustrate our meta-learning method using machine learning (ML) based on reservoir computing, we emphasize that the general technique – combining short time series data from the system of interest with much more extensive data from related systems through a two-level meta-learning process – can be applied to other ML approaches with memory. These approaches will differ in the structural representations of both the ML model parameters for the library members and the encoded memory needed for cold-starting. Hence, the primary distinction in implementing METAFORS with different ML types is that the signal mapper must be trained on the different representations of model parameters and cold-start vectors. However, we do not anticipate this to present a fundamental challenge for implementing a METAFORS scheme. Furthermore, the method is also applicable to memoryless ML types, which could be relevant in cases where the time-series of the full state of the system is measured for both training and test signals. In the memoryless case, the cold-start vectors are not needed, and the METAFORS implementation simplifies significantly, as the signal mapper only has to map to the model parameters.

II. RESULTS

In this section, we first outline our reservoir computing implementation of METAFORS, leaving a more detailed description to Section IV. Then we use this implementation to show that METAFORS can generalize from a library of machine learning (ML) forecasting models to create tailored forecasts for test systems for which the dynamics are unknown and the available data are insufficient to train the forecaster directly. Our tests make use of data from three commonly studied nonlinear systems: the logistic map⁵⁴, the Gauss iterated map⁵⁵, and the Lorenz-63 equations⁵⁶.

A. Implementation overview

The central component of a reservoir computer (RC) is a recurrent neural network, referred to as a reservoir. Each node in the reservoir network has an associated continuous-valued activation level, and the collection of all the node activations at a given time constitutes the state of the reservoir at that time, $\mathbf{r}(t)$. The reservoir state evolves over time in response to an external input signal, $\mathbf{u}(t)$, and is influenced, at every time step, by its own state at the previous time step via directed interactions between its nodes. This recurrence gives the reservoir ‘memory.’ We generate ‘outputs,’ $\hat{\mathbf{u}}(t)$, of the reservoir by forming linear combinations of the reservoir

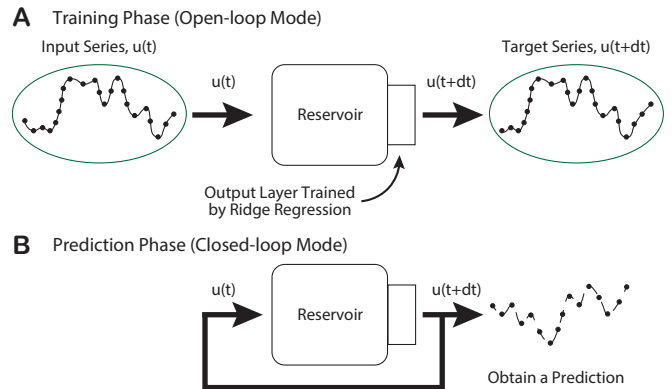


FIG. 2: A Reservoir Computer for Time Series Prediction

nodes’ activations, or, equivalently, applying a linear operator to the reservoir state vector. In this work, we train a forecaster RC for time series prediction by driving it with a training signal in ‘open-loop’ mode (Fig. 2A) and then choosing this linear operator, or ‘output layer’, such that the outputs at each time step closely match the target at the next time step, $\hat{\mathbf{u}}(t) \approx \mathbf{u}(t + \Delta t)$. We make this choice by simple linear regression and use a regularization parameter to prevent overfitting. To make a prediction, we feed the RC’s output back as its input at each time step and it evolves as an autonomous dynamical system in ‘closed-loop’ mode (Fig. 2B). The RC’s output layer determines the dynamics of this autonomous system and its internal state, $\mathbf{r}(t)$, determines its position in the phase space of those dynamics. Typically, to initialize a forecast, we must synchronize the reservoir state to the test system by driving the RC in open-loop mode with a time series immediately preceding the start of the forecast. If the available time series is too short, the forecast will be inaccurate even if the RC’s output layer accurately represents the relevant dynamics. This is because the reservoir state contains memory about previous inputs, so it requires a sufficient ‘synchronization time’ to properly initialize its memory.

We build METAFORS’ library of long time series and associated trained ML models as follows. First, we train the forecaster on each available long signal as above. Through this process, we obtain, for each long signal, a well-trained output layer and well-synchronized reservoir states at every time step. The output layer constitutes the forecaster’s trained parameters, θ , and its reservoir state at time t constitutes a cold-start vector for a test signal starting at time t , $\mathbf{m}(t) \equiv \mathbf{r}(t)$. We train the signal mapper, which is also an RC in our implementation (but could easily be constructed by other ML schemes), to map each short signal extracted from the library to the reservoir state corresponding to its start and the output layer trained on the long signal from which it was extracted. In the prediction phase, the signal mapper learns, from a given test signal, an output layer for the forecaster and a cold-start vector corresponding to the start of the test signal. To mitigate errors in the learned cold-start vector, we then synchronize the forecaster to the test signal using this cold-start vector as the forecaster’s initial reservoir state. Finally, the forecaster evolves autonomously from the end of the test signal to gen-

erate a forecast.

Once we have obtained a forecast, we can quantify its short-term accuracy by measuring its valid prediction time

$$T_{valid} = \min \left\{ t - t_{test} : \left\| \frac{\hat{\mathbf{u}}(t) - \mathbf{u}(t)}{\text{std}(\mathbf{u})} \right\| > 1 \right\}, \quad (1)$$

where the test signal, of N_{test} sequential observations, starts at $t = 0$ and the prediction starts at $t_{test} \equiv (N_{test} - 1)\Delta t$. $\hat{\mathbf{u}}$ and \mathbf{u} are the predicted and true signals, respectively, and $\text{std}(\mathbf{u})$ denotes the standard deviation of \mathbf{u} over time. Both $\text{std}()$ and division are performed in a component-wise manner.

We quantify how faithfully a forecast captures the long-term statistics, or climate, of a test system, with the autonomous one-step error⁵⁷:

$$\varepsilon = \langle \|\mathbf{P}[\hat{\mathbf{u}}(t)] - \mathbf{F}[\hat{\mathbf{u}}(t)]\| \rangle. \quad (2)$$

Here, $\hat{\mathbf{u}}(t)$ is the predicted system state at time t and $\langle x \rangle$ denotes the time-average of x over the forecast period. $\mathbf{F}[v]$ and $\mathbf{P}[v]$ are functions that evolve the system state v at time t forward to time $t + \Delta t$ according to the true system dynamics, and those learned by the forecasting model, respectively; i.e., if $\mathbf{u}(t)$ is the true system state at time t , $\mathbf{F}[\mathbf{u}(t)] = \mathbf{u}(t + \Delta t)$, by definition. The autonomous one-step error is defined only for forecasts of the full system state.

B. Framework and rationale for experiments with simulated data

To test the effectiveness of METAFORS, we use toy chaotic systems as a controlled experimental testbed. These systems are widely studied in nonlinear dynamics because they exhibit rich, complex behaviors despite being governed by relatively simple equations. Their simplicity allows for systematic generation of ground truth data and facilitates evaluation of forecasting performance over broad ranges of their dynamical parameters. Their capacity to exhibit qualitatively different behaviors with different values of their parameters makes them ideal for probing how system-relatedness, test signal length, and library data coverage influence the ability of METAFORS to construct tailored forecasts.

For the scenarios we consider, the data for both the long library signals and the short test signals are discrete in time. This discreteness arises either because of sampling in the case of predicting the evolution of continuous time systems, where we denote the sampling interval as Δt (and take the ML prediction time step to also be Δt), or because the system itself evolves in discrete time, as with the logistic map (Section II C). For continuous time systems, Δt can be short compared to the system's characteristic time scales (e.g., its Lyapunov time). By contrast, for discrete time systems, the time step is typically on the scale of the system's evolution dynamics. A key challenge for ML prediction from short-duration time series lies in the insufficient sampling of the dynamics on the unknown attractor. Short signals may fail to capture the system's full range of behaviors, making it difficult to accurately approximate functions that govern the dynamics. Fundamentally, learning the system's dynamics may be thought

of as equivalent to learning functions — e.g., for a system of ordinary differential equations, $dx/dt = \mathbf{F}(x)$, learning \mathbf{F} , or, for a discrete-time system, $x_{n+1} = \mathbf{M}(x_n)$, learning \mathbf{M} . METAFORS addresses this issue by utilizing information learned from systems with similar functions \mathbf{F} or \mathbf{M} for which more extensive data are available.

We first test METAFORS in an idealized scenario where both the library members and the test signals are drawn from the same dynamical system family (the logistic map; Section II C). Even in this case, where dynamics are governed by a simple quadratic equation, baseline ML approaches that assume no knowledge of the governing equations struggle to generalize effectively. By combining short test signals with information from the library, METAFORS substantially improves forecast quality, even when the test and library signals are generated from different ranges of the bifurcation parameter so that their underlying dynamics differ significantly.

In Section II C, we draw the library members and test signals from two distinct families of dynamical systems, the logistic map and the Gauss iterated map, and show that METAFORS can implicitly determine the system type from a short test signal and build tailored forecasters in parameter regions not covered in the library.

Finally, in Section II E, we demonstrate that METAFORS can amalgamate the information in the test and library signals to improve forecast quality even when each signal contains only partial information of the state of the system that generated it.

We emphasize that every library member in METAFORS consists of a long training signal and its corresponding ML model representation only. To present results in pictorial form and to discuss parameter-aware benchmark methods, we frequently refer to the dynamical parameters used to generate the long library signals and short test signals. These parameters are not, however, included in METAFORS' library and METAFORS does not have access to them or use them to make forecasts.

C. Employing METAFORS to generalize the logistic map

We employ the logistic map⁵⁴ as a simple test bed to demonstrate that METAFORS can generalize our RC forecaster to capture the long-term statistics, or climate, of trajectories with qualitatively different behaviors. The logistic map,

$$x_{n+1} = rx_n(1 - x_n) \quad (3)$$

is a simple model of population dynamics. The variable x represents the current population of a species as a fraction of its maximum possible population. When x is small, it grows approximately proportionally to itself at the reproduction rate, or logistic parameter, r ; when x is large, the population declines proportionally to r because resources are scarce. The map is of interest to us, and is commonly studied in dynamical systems, because it exhibits sudden transitions between qualitatively different behaviors as the value of r changes. Here, we focus on the range $2.9 \leq r \leq 4$. For $2.9 \leq r < 3$, the map has

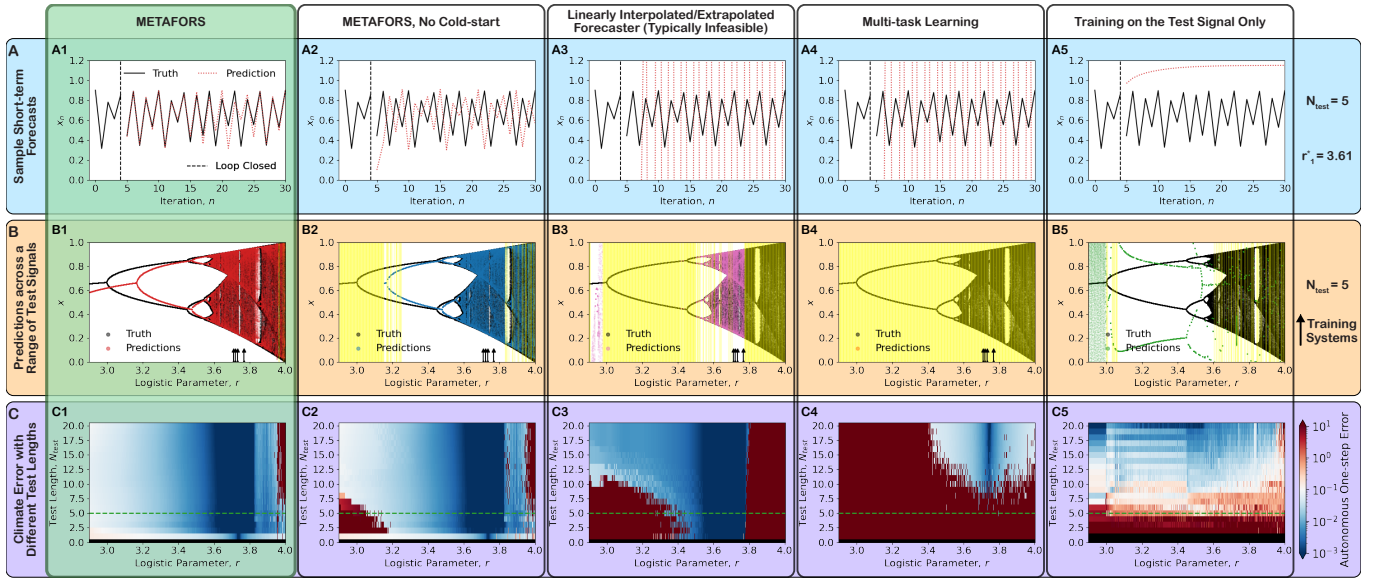


FIG. 3: Trained on just five stationary signals, METAFORS can replicate the logistic map’s dynamics across a large portion of its bifurcation diagram from short test signals with unknown dynamical parameters.

We train METAFORS on a library of five trajectories from the logistic map with logistic parameters chosen randomly from $3.7 \leq r \leq 3.8$. All signals in the library are chaotic; periodic trajectories are excluded from selection. **(A)** Short-term forecasts from a sample short test signal of length $N_{test} = 5$ with logistic parameter $r_1^* = 3.61$. **(B)** Bifurcation diagrams constructed by METAFORS and baseline methods with test signals of length five iterations. Black arrows indicate the logistic parameters of the long library signals. Vertical yellow lines indicate values of r for which the corresponding forecast leaves the basin of attraction $0 \leq x \leq 1$ and does not return. **(C)** Climate replication, measured by the autonomous one-step error, at test lengths $1 \leq N_{test} \leq 20$ for each method. For each grid point, we record the median autonomous one-step error over 10 random realizations of the forecaster and signal mapper reservoirs, and of the initial conditions of the long signals in the library. The dynamical parameters of the library signals in all realizations are the same as depicted in panel **(B)**. Green horizontal lines indicate the test length used in panels **(A)** and **(B)**. In the true bifurcation diagram **(B)**, we plot, for each of 500 evenly-spaced values of $2.9 \leq r \leq 4$, the final 500 iterations of a trajectory of total length 2000 iterations starting from a randomly chosen initial condition $0 < x_0 < 1$. We start each prediction at iteration 1000 of the corresponding true trajectory and discard the first 500 predicted iterations to ensure that the forecast long-term climate is not obscured on the plot by any initial transient behavior. We plot the subsequent 500 predicted iterations. Similarly, we use the final 500 predicted iterations to calculate the autonomous one-step error in the heatmaps **(C)**.

a single stable fixed point, to which trajectories from all initial conditions in the interval $0 < x_0 < 1$ converge. At $r = 3$, the first bifurcation in a period-doubling cascade occurs as trajectories transition first to a period-2 orbit and then to periodic orbits of increasing period. Chaotic, aperiodic behavior sets in at $r \approx 3.569$ and is interspersed by windows of periodic orbits as r increases through $3.569 \lesssim r \leq 4$. We illustrate this period-doubling cascade as the black *Truth* background of the bifurcation diagrams in Fig. 3.

We consider each logistic map with a fixed value of r as a distinct dynamical system. To demonstrate that METAFORS can capture the climate of unseen test systems with qualitatively different behaviors, we train it on a small number of dynamical systems from the logistic map and show that it can recover a broad portion of the map’s bifurcation diagram. More precisely, we build a library containing five ML models, each trained on a long trajectory of a chaotic logistic map with logistic parameter drawn randomly from the interval $3.7 \leq r \leq 3.8$, excluding values for which the dynamics are periodic. (See Section IV C 1 for details.) We then make predictions with short test signals from 500 unseen systems with

values of r evenly-spaced over $2.9 \leq r \leq 4$. It is necessary to exclude periodic trajectories from the training library because they poorly sample the phase space of the logistic map. A non-parametric forecasting model, such as an RC, trained on an orbit with a short periodicity length may not learn a sufficiently complex representation of the dynamics. As a result, its inclusion in the training library may hamper generalization.

We compare METAFORS’ reconstruction to those of four other methods. In *METAFORS, No Cold-start*, we use the signal mapper only to learn parameters for the forecaster, not to cold-start it. Instead, we initialize the forecaster’s internal state for prediction by driving it, from a zero-vector initial state, with the test signal as input. The *Interpolated/Extrapolated Forecaster* (Section IV D 3), relies on knowledge of the logistic parameter’s value for each of the training and test systems. We identify, for each test system, the library members whose associated values of the logistic parameter are closest to that of the test system. Then we perform element-wise linear interpolation or extrapolation of model parameters from the library, depending on whether the test system is within or beyond the range of the library. Inter-

polation and extrapolation are not feasible when knowledge of the dynamical parameters of the training and test systems is not available. In our simple *Multi-task Learning* approach (Section IV D 2), we train a single forecaster RC on the union of all long signals in the library. In *Training on the Test Signal Only* (Section IV D 1), we train a separate forecaster RC directly on each short test signal. For all of these methods, we first drive the forecaster with the test signal starting from a zero-vector initialization to try to synchronize its internal state to the test signal before closing the loop and making predictions, as in *METAFORS, No Cold-start*.

In Fig. 3(A) we plot short-term forecasts obtained with each of these methods from a short test signal with sample value of the logistic parameter $r_1^* = 3.61$. Only METAFORS' forecast is accurate. In Fig. 3(B), we use the same methods to construct bifurcation diagrams of the logistic map from test signals of just five iterations ($N_{test} = 5$). In particular, we generate the test signals by iterating the logistic map with different values of its bifurcation parameter sampled uniformly over a wide range. We then provide each test signal to the forecasting method of choice and construct the corresponding bifurcation diagram by plotting the long-term predictions of the system's state as a function of the bifurcation parameter r . These diagrams reveal several noteworthy features. First, Fig. 3(B1) shows that METAFORS successfully captures the logistic map's dynamics over a broad range of its bifurcation parameter, demonstrating robust performance. (We note that METAFORS exhibits strong performance even when the test signal is as short as two iterations – see Fig. 9. We display results for $N_{test} = 5$ here so as to illustrate some regions where the other methods succeed.) Second, by comparing panels (B1) and (B2), we can see that the cold-start vectors that METAFORS learns are important when the test signals are very short. With test signals of five iterations, only METAFORS' forecasts remain bounded across the whole test set. Both the linearly interpolated/extrapolated forecasters and those constructed, but not cold-started, by METAFORS replicate the dynamics of the logistic map well over portions of the bifurcation diagram but predict divergent trajectories for many values of r . The difference in performance between METAFORS and these methods highlights that cold-starting presents a challenge to memory-based forecasters even when the goal is solely to predict a test system's long-term climate rather than its short-term evolution. If not suitably initialized, even a well-trained forecaster may end up in a basin of attraction that is inconsistent with the true system. METAFORS mitigates this issue effectively.

Fig. 3(B5) demonstrates that test signals of five iterations are too short for RC forecasters trained directly on the test signals to learn the dynamics of the logistic map well, even though the logistic map is governed only by a simple quadratic equation. In Fig. 3(C), we plot the autonomous one-step error of the forecasts from each of our methods with test signals of different lengths. METAFORS captures the climate of test systems with unseen logistic map dynamics more accurately than all of our baseline methods for test signals of length $N_{test} \leq 20$ iterations. Panel (C4), on the other hand, demonstrates that even when the test signals are long enough

to initialize the forecaster well without METAFORS' cold-starting, our simple multi-task learning approach to training the forecaster offers good climate replication only when the logistic parameter of the test system is quite close to those of the library members. Once trained by this method, the forecaster can capture varied dynamics only if its internal basin structure is sufficiently complex to accommodate attractors of distinct dynamical systems simultaneously and access their corresponding basins through suitable initialization with a test signal⁴¹. Otherwise, its fixed model parameters can represent just one dynamical system, typically some kind of average of the systems seen in training. (We note that recent work has explored the problem of representing varied dynamics with a single trained ML model in the context of parameter-aware forecasting^{26–30,42}.)

Finally, we emphasize that METAFORS is unaware of the logistic parameters of the training or test systems. While linear interpolation/extrapolation of the forecaster parameters performs comparably to METAFORS once the test signals are long enough, it requires knowledge of the underlying dynamical parameters and is thus typically infeasible in scenarios of interest.

D. Simultaneous learning and generalization of logistic and Gauss iterated maps

To extrapolate beyond the domain of the training data is often a significant challenge for ML models. In Fig. 3, however, METAFORS extrapolates to test systems with dynamical parameters that are far from those of the library signals. This surprising range may be due, at least in part, to the fact that the logistic map is itself linear in r . (Note that linear extrapolation of the forecaster parameters also captures well the dynamics of systems far from the library.) METAFORS' performance in Fig. 3 is further aided by the library's construction: by training METAFORS on dynamical systems from the logistic map only, we constrain the space of dynamics over which the signal mapper must learn suitable forecaster parameters and cold-start vectors. In this section, we demonstrate that METAFORS can generalize the forecaster to: (a) test systems governed by a map that is nonlinear in its bifurcation parameter, and (b) cases where the training and test signals originate from dynamical systems with distinct functional forms.

The Gauss iterated map, or mouse map, is given by

$$y_{n+1} = e^{-ay_n^2} + b. \quad (4)$$

Like the logistic map, its dynamics undergo bifurcations and exhibit qualitatively different behaviors as its parameters, a and b , vary.

We demonstrate in Fig. 4 that METAFORS can learn to represent dynamical systems from both the logistic and Gauss iterated maps simultaneously. We train METAFORS on a library of ten long series: five from the logistic map with parameter r randomly chosen from $3.6 \leq r \leq 3.9$, and five from the Gauss iterated map with the drift parameter $b = -0.5$ and randomly chosen values of the exponential parameter $6 \leq a \leq 12$, excluding periodic trajectories as in Section II C (Fig. 4A). To

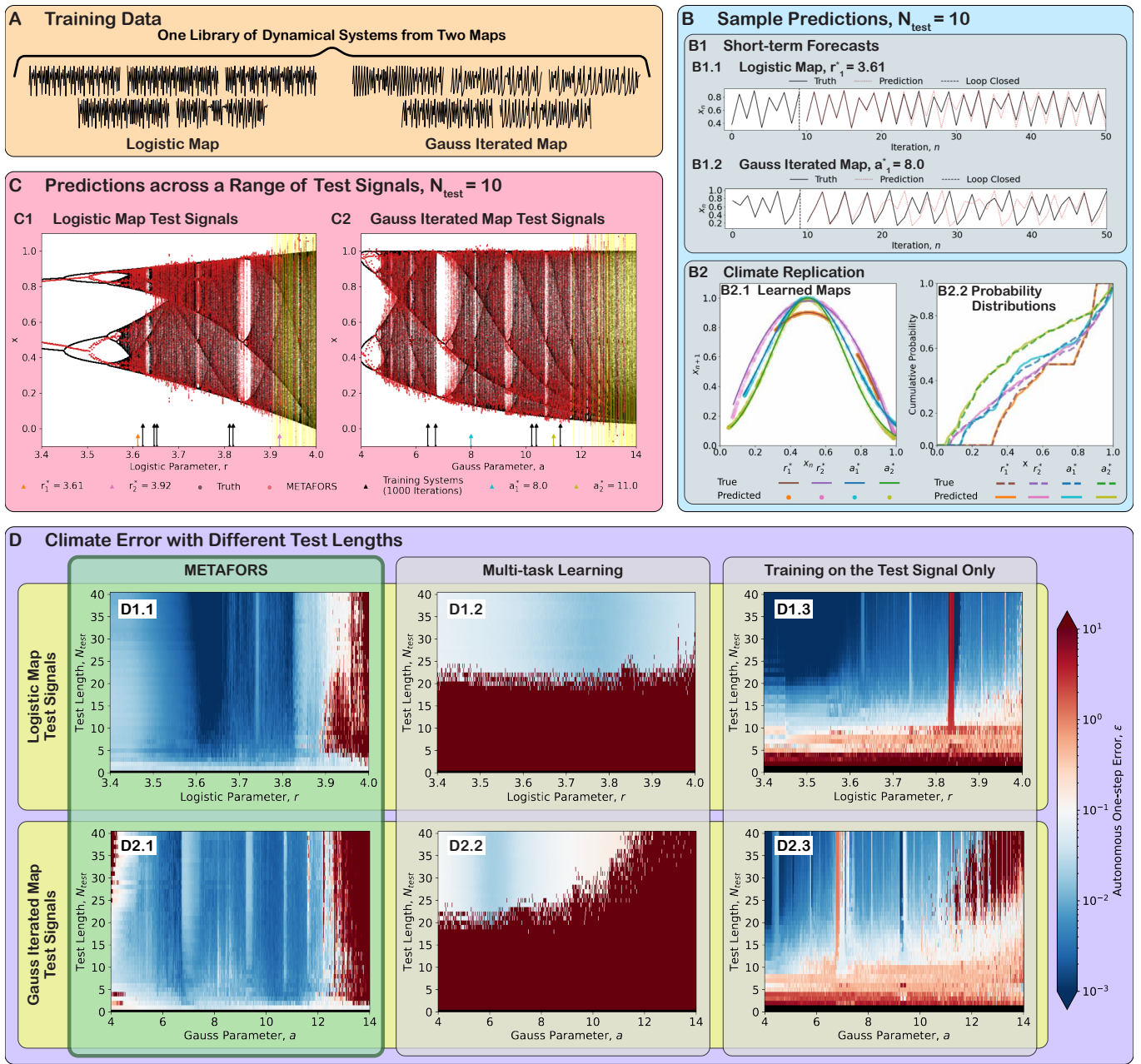


FIG. 4: METAFORS can learn to represent dynamical systems of distinct functional forms simultaneously.

We train METAFORS on a library of ten trajectories: five from the logistic map with logistic parameters chosen randomly from $3.6 \leq r \leq 3.9$ and five from the Gauss iterated map with exponential parameters chosen randomly from $6 \leq a \leq 12$. All ten signals in the library are chaotic; periodic trajectories are excluded from selection. **(A)** The first 100 iterations of each long library signal, of total length 1000 iterations. **(B1)** Short-term forecasts obtained with METAFORS at sample parameter values. **(B2)** METAFORS' climate replication demonstrated by the one-step update map it learns **(B2.1)** and the cumulative probability distribution of its predicted trajectories **(B2.2)** at sample parameter values $r_1^* = 3.61$, $r_2^* = 3.92$, $a_1^* = 8$, and $a_2^* = 11$. **(C)** The true and learned bifurcation diagrams of the logistic map **(C1)** and the Gauss iterated map **(C2)**. There are 500 test signals of length $N_{test} = 10$ iterations for each map. They are spaced evenly over $3.4 \leq r \leq 4$ for the logistic map and over $4 \leq a \leq 14$ for the Gauss iterated map. **(D)** Median autonomous one-step error, calculated over ten random realizations of the forecaster and signal mapper RCs' internal connections and the initial conditions of the long library signals, for METAFORS, Multi-task Learning, and *Training on the Test Signal Only*, with test signals of different lengths from both maps. Black regions at $N_{test} = 0$ for all methods and at $N_{test} = 1$ for *Training on the Test Signal Only* indicate that no prediction can be obtained. For all panels, the predicted and true trajectories are 500 iterations long and the training library is the same one that is plotted in **(A)** and depicted as black arrows in **(B)**.

make the task of differentiating between trajectories from both maps more challenging, we translate trajectories of the Gauss iterated map as

$$x_{n+1} = y_{n+1} - b, \quad (5)$$

so that the distributions of states visited by each map overlap substantially. The trajectories from both are confined to, and cover well, the interval (0,1). This overlap ensures that METAFORS cannot, for instance, learn to identify with the Gauss iterated map all test signals that have a negative entry.

In Fig. 4(B), we demonstrate that METAFORS captures both the short-term evolution (B1) and long-term climate (B2) of specific sample systems from the chaotic regimes of each map with test signals of only $N_{test} = 10$ iterations. Fig. 4(B2.1) shows that the maps traced out by the true and predicted trajectories of the sample systems agree closely and Fig. 4(B2.2) plots the cumulative probability distributions of states visited by the same trajectories. Fig. 4(B2) makes clear the high degree of overlap in the distributions of the logistic and translated Gauss iterated maps. It also demonstrates that METAFORS nevertheless predicts the state distributions of our sample test systems accurately, and successfully distinguishes between test signals from each map with very limited data.

In Fig. 4(C), we forecast from 500 short test signals, of length $N_{test} = 10$ iterations, at evenly-spaced values of each map’s bifurcation parameter and see that METAFORS can indeed capture the climate of test systems from both maps over a broad range of their bifurcation diagrams. (Note that while we use knowledge of the bifurcation parameters of the training and test signals to construct the bifurcation diagrams, METAFORS has no access to, and does not use, this knowledge when generating forecasts.) While METAFORS does miss some features of the bifurcation diagrams – for example, it predicts that the bifurcation of the logistic map from a period-2 orbit to a period-4 orbit occurs at $r \approx 3.5$ instead of $r \approx 3.45$ – its reconstructions are broadly accurate. Finally, in Fig. 4(D) we compare METAFORS’ climate replication across both maps’ bifurcation diagrams to two other methods – an RC forecaster trained by multi-task learning and RC forecasters trained directly on the short test signals – with test signals of different lengths.

We emphasize again that METAFORS has no awareness of the parameters that govern the dynamics of the training or test systems. Moreover, it is not explicitly aware of which map has generated any given signal. METAFORS infers the relevant dynamics from the observed test signal alone. Parameter-aware generalization methods, such as simple interpolation/extrapolation, are not readily applicable to this problem. To use such methods, we would require an additional input channel to indicate which parameter a supplied value measures.

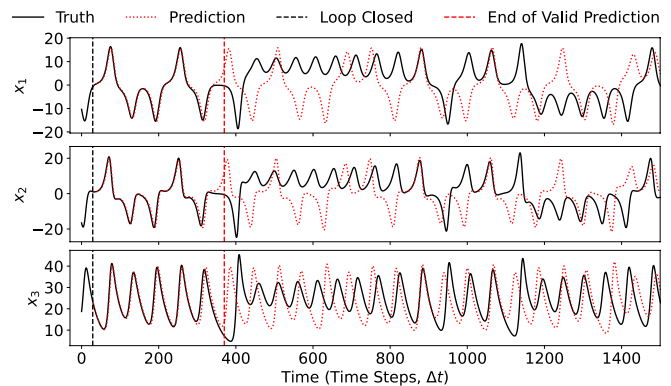


FIG. 5: An example Lorenz-63 forecast using METAFORS The test signal, of $N_{test} = 30$ sequential points, is the segment of the true signal before the vertical dashed black line at $t_{test} \equiv (N_{test} - 1)\Delta t$. The forecast starts at t_{test} and yields a valid prediction time $T_{valid} = 340\Delta t$, as defined by Eq. (1). The parameters of the $N_L = 9$ long library signals are as shown in Fig. 6. They were selected randomly from the uniform distributions $\omega_r \in U[0.75, 1.25]$ and $v_1 \in U[7.5, 12.5]$, as in Section IV C 2. The Lorenz parameters of the test system are $(\omega_r, v_1) \approx (1.25, 10.83)$.

E. Generalization in fully and partially observed Lorenz-63 systems

While we believe that larger applications like weather forecasting could benefit from the approaches used in METAFORS, here we employ a simplified but widely studied model of atmospheric convection, the Lorenz-63 equations⁵⁶, as another test bed for METAFORS. First, we briefly demonstrate that METAFORS’ forecasts capture the climate of test systems with unseen Lorenz-like dynamics, and then we use METAFORS to predict the short-term evolution of such systems in a few distinct scenarios. Of particular note, we show that METAFORS can still generalize and cold-start the forecaster when only partially-observed states of the training and test systems are available. Partial-state forecasting is required in many applications – especially those where the system of interest is high-dimensional and only a few variables can be feasibly measured, such as in weather-forecasting and epidemiology.

Lorenz systems are governed by three ordinary differential equations:

$$\dot{x}_1 = \omega_r [v_1(x_2 - x_1)], \quad (6a)$$

$$\dot{x}_2 = \omega_r [x_1(v_2 - x_3) - x_2], \quad (6b)$$

$$\dot{x}_3 = \omega_r [x_1 x_2 - v_3 x_3]. \quad (6c)$$

Each set of values of the parameters ω_r , v_1 , v_2 , and v_3 define a unique dynamical system. For our experiments, every long library signal and short test signal is a segment of the attractor of a Lorenz system with different values of the parameter v_1 and the time-scale, ω_r . We hold $v_2 = 28$ and $v_3 = 8/3$

fixed. The factor ω_t does not appear in the original formulation of the equations, but allows for changes to the time-scale of chaotic oscillations. Increasing ω_t causes a system to evolve more rapidly with time.

For all values of the Lorenz parameters that we explore here, the equations exhibit chaotic dynamics: any two trajectories will become decorrelated after a finite time, regardless of how close their initial conditions are. We can quantify the time-scale over which a system’s underlying chaotic dynamics make prediction impossible using Lyapunov times⁵⁸. A Lyapunov time is the time required for the distance between two trajectories that are initially close together to increase by a factor of Euler’s number, e . A system’s Lyapunov time scales proportionally to ω_t . We therefore measure periods of time in units of our constant time step, $\Delta t = 0.01$, to report results. For context, however, we note that the Lyapunov time of the Lorenz system with standard parameter values $\omega_t = 1$, $v_1 = 10$, $v_2 = 28$, and $v_3 = 8/3$ is $\tau_{Lyap} \approx 1.104 \approx 110\Delta t$. Because we use a constant time step, by varying ω_t we vary how finely the data are sampled.

In our experiments with fully-observed Lorenz systems, we train the forecaster RC to take as input and predict as output the full system state (x_1, x_2, x_3) at each instant. For our experiments with partially-observed Lorenz systems, the forecaster is trained on and predicts the x_3 -component only. Full details of the experimental parameters defining METAFORS’ library and training scheme for our experiments with Lorenz systems are given in Section IV C 2. An example forecast of a fully-observed Lorenz system using METAFORS is shown in Fig. 5. Note that the test signal starts at time $t = 0$ and the first predicted data-point is at $t = t_{test}$. For clarity, we follow this convention always. The valid time is measured as in Eq. (1).

1. METAFORS captures both the climate and short-term evolution of unseen Lorenz systems

In Fig. 6, we present results for a library constructed from nine Lorenz systems with different parameter values, illustrating how the long-term climate replication (A) and short-term forecast accuracy (B), measured by the autonomous one-step error and valid prediction time, respectively, vary with the test parameters v_1 and ω_t . We compare METAFORS’ generalization ability to a few simple baseline approaches. First, for the *Nearest Library Forecaster*, we rescale the dynamical parameters ω_t and v_1 used to generate the long library signals such that they span a unit interval along both axes. Then, for each test signal, we make a prediction using the forecaster RC of the long library signal whose re-scaled dynamical parameters are nearest to those of the test system. We emphasize that in typical applications we do not know the dynamical parameters associated with either the short test signals or the long library signals, so this comparison is typically infeasible. For the *Interpolated Forecaster* (Section IV D 3), we perform linear interpolation of the forecaster model parameters if the test system lies within the convex hull of the library. Otherwise, we use the forecaster RC of the nearest library member. We choose this interpolation/extrapolation method because it is

applicable to high-dimensional spaces and assumes no underlying structure in the distribution of the library members, but more sophisticated schemes may offer better performance. As with the nearest library forecaster, we note that interpolation of the model parameters is typically infeasible. We include it here as a comparison to a scheme that relies on additional information (i.e., the typically unknown dynamical parameters). Since no cold-start vector is learned in either of these methods, or in our simple multi-task learning approach, we obtain forecasts by synchronizing the forecaster to the test signal from a zero-vector internal state, $\mathbf{r}(0) = \mathbf{0}$, before prediction begins at $t = t_{test}$.

Fig. 6(A1) and (B1) illustrate the brittleness of the RC forecasting models in our library. Each forecaster model in the library provides strong climate replication (A1) and accurate short-term forecasts (B1) only if the test signal parameters are very close to those of the system on which it was trained. Panel (A4), on the other hand, demonstrates that our basic multi-task learning approach to training the forecaster fails to capture the climate of unseen test systems even when their dynamical parameters are quite close to those used in the library. The multi-task learning approach is slightly more useful for short-term forecasting (B4), but struggles in a way that is common to multi-task learning methods: by training to improve performance on the library members generically, it does not forecast any single system accurately. We show in Fig. 10 that a larger (i.e., more powerful) multi-task forecaster RC does not close the performance gap between the basic multi-task learning method and METAFORS. Panels (A3) and (B3) demonstrate that METAFORS facilitates the generalization that is required for this problem. Over a wide range of test signal dynamics, METAFORS offers lower autonomous one-step errors (A3) and higher valid prediction times (B3) than the other methods. In particular, METAFORS offers longer valid prediction times than does the parameter-aware *Interpolated Forecaster* (B2) method unless the test dynamics are very similar to the dynamics of one of the library members.

Fig. 11 explores further how the library structure (i.e., the length and number of library signals) affects METAFORS’ performance.

2. With very short test signals, METAFORS’ cold-starting is essential

We plot mean valid prediction time against test signal length for METAFORS and a few baseline methods in Fig. 7. Here, both the training and test signals contain only partially-observed Lorenz states (the x_3 -component only). We present similar results with fully-observed Lorenz systems in Fig. 12. METAFORS’ ability to cold-start forecasts strikingly increases valid prediction times when the test signals are short. With test signals of length $t_{test} = 19\Delta t$ ($N_{test} = 20$), for instance, METAFORS’ mean valid prediction time, $T_{valid} \approx 139\Delta t$, is just over seven times the length of the test signals. All other methods synchronize the forecaster RC to the test signal from a zero-vector internal state $\mathbf{r}(0) = \mathbf{0}$ and thus cannot offer useful forecasts until the duration of the

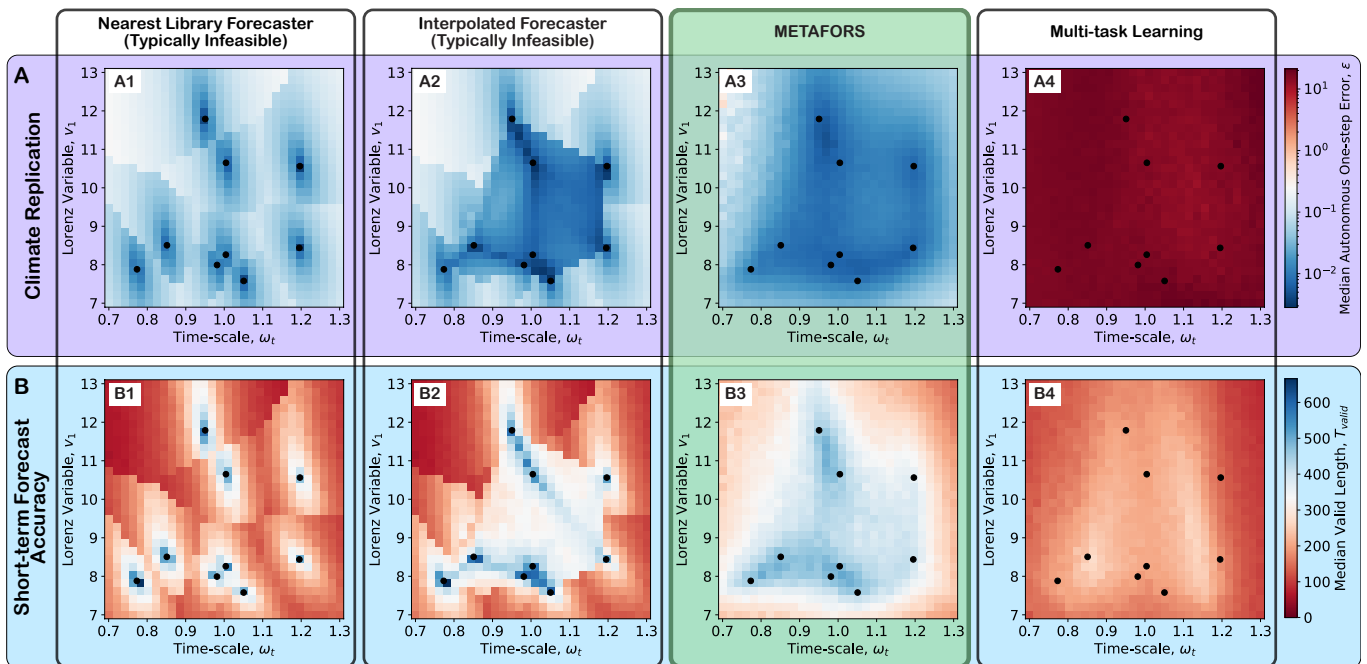


FIG. 6: **METAFORS generalizes the forecaster to Lorenz-like dynamics unseen in the library.**

The Lorenz parameters of the long library signals, marked by black dots, were randomly selected from the uniform distributions $\omega_t \in U[0.75, 1.25]$ and $v_1 \in U[7.5, 12.5]$, as in Section IV C 2. The library and test signals contain observations of the full state of the Lorenz system. **(A)** At each grid point, we calculate the mean autonomous one-step error, which measures climate reproduction, for each of 500 forecasts of duration $3000\Delta t$, and then plot the median of these means. **(B)** The median valid times, which measure short-term prediction accuracy, for the same set of forecasts. In **(A1)** and **(B1)**, we use the forecaster of the library member closest in (ω_t, v_1) -parameter space to the test signal. In **(A2)** and **(B2)**, we triangulate the parameter values $(\omega_t^{test}, v_1^{test})$ of each test system with respect to the Lorenz parameter values of the library members. If the test parameters lie inside the convex hull of the long library signals, we calculate the output layer of the forecaster RC by interpolation of the three closest library members. Otherwise, we use the nearest library forecaster. The test length, $N_{test} = 200$, is longer than the memory of the forecaster, so that the cold-start vector learned by METAFORS offers no advantage.

test signal is comparable to that of the forecaster’s memory. When the test signals are long enough that cold-starting is not required, METAFORS’ valid prediction time still settles at a higher plateau value than even our parameter-aware *Interpolated Forecaster* method, the best performing of the baseline approaches considered. The poor performance of forecaster RCs trained directly on the test signals (*Train on Test Signal*), in contrast, highlights that even these longest test signals are significantly shorter than is required to train a forecaster RC accurately.

3. METAFORS is useful for cold-starting even when generalization is not required

While we typically do not expect ML forecasting models trained on data from one dynamical system to generalize well to test systems with different dynamics, we do expect that a forecaster should offer useful predictions for test signals that exhibit identical dynamics to those of its training system. ML forecasters with memory, however, struggle in this scenario unless the test signal is sufficiently long to initialize their memory.

In Fig. 8, we train METAFORS on a single long library signal with standard Lorenz parameters $\omega_t = 1$ and $v_1 = 10$ and test it on short signals with the same dynamics starting from 625 different initial conditions. Since there is only one training time series, the signal mapper only has to map short signals to cold-start vectors, with the forecaster’s model parameters determined by training on the sole long library signal. In both the partially-observed (Fig. 8) and fully-observed (Fig. 12(B)) forecasting tasks, METAFORS’ signal mapper enables simple cold-starting of the forecaster. We emphasize that the signal mapper requires no more training data than is traditionally required for forecasting of stationary dynamics; it is trained from the same data as the forecaster in order to cold-start predictions at new points in phase space.

The utility of METAFORS’ cold-starting in this simplified setting is highlighted by comparison to the traditional approaches that we include as baseline methods in Fig. 8. For the method labeled $r(0) = 0$, we synchronize the forecaster to each test signal starting from a zero-vector internal state before prediction begins. This is a typical approach for initializing a memory-based forecaster. In *Backward Extrapolation as a Constant*, we extrapolate the test signal backwards from its initial value, $s_{test}(0)$, as a constant for two-hundred time

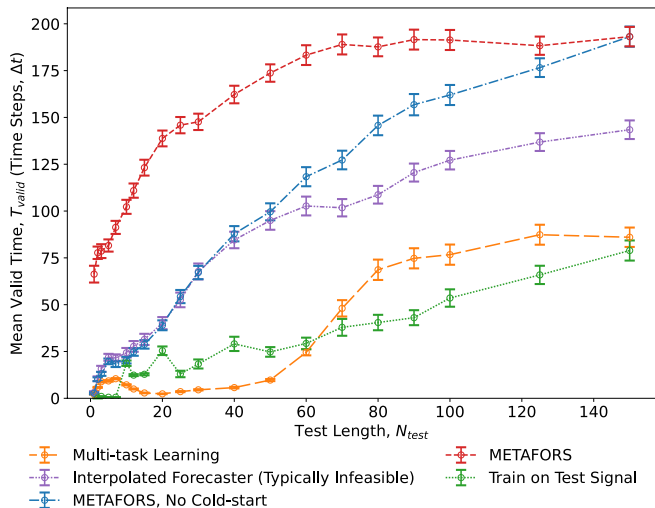


FIG. 7: **METAFORS forecasts partially-observed Lorenz systems from very limited data.** Using a library comprising $N_L = 9$ long signals with Lorenz parameters indicated by the black dots in Fig. 6, we calculate mean valid times over 625 test signals arranged in a 25×25 rectangular grid spanning the space defined by $0.7 \leq \omega_t \leq 1.3$ and $7 \leq v_1 \leq 13$. The training and test signals contain only the x_3 Lorenz variable. Error bars denote the standard error of the mean. For *METAFORS, No Cold-start* (blue), the signal mapper RC learns model parameters but no cold-start vector for the forecaster. For that method and all others except *METAFORS*, we synchronize the forecaster to the test signal from a zero-vector internal state, $\mathbf{r}(0) = \mathbf{0}$, and then predict in autonomous/closed-loop mode (Fig. 2B) from the end of the test signal.

steps and then synchronize the forecaster to this extrapolated signal

$$\mathbf{s}_{test}^{extrap}(t) = \begin{cases} \mathbf{s}_{test}(0), & -200\Delta t \leq t < 0 \\ \mathbf{s}_{test}(t), & 0 \leq t \leq t_{test} \end{cases},$$

starting from $\mathbf{r}(-200\Delta t) = \mathbf{0}$. In *Training Data Search*, we search the training series for the segment, s_{match} , that minimizes the root-mean-square error between the test signal and itself. Denoting by $\mathbf{r}_{train}(t_{match})$ the constructed cold-start vector at the time step of the training signal at which s_{match} begins, we then synchronize the forecaster to the test signal starting from the initial state $\mathbf{r}(0) = \mathbf{r}_{train}(t_{match})$. This method of searching the library for the closest match to the test signal offers considerable improvement over the two other traditional approaches that we highlight, but it requires a computationally expensive search each time we wish to make a new prediction. Its performance may also depend on how well the training signal covers its associated attractor. *METAFORS*, on the other hand, can learn a cold-start vector cheaply for each test signal – no retraining of the signal mapper is required.

We make two brief technical observations. *METAFORS*' peak valid prediction time in Fig. 7 is significantly lower than it is in Fig. 8, where we do not require generalization to new dynamics. This discrepancy is related to training regu-

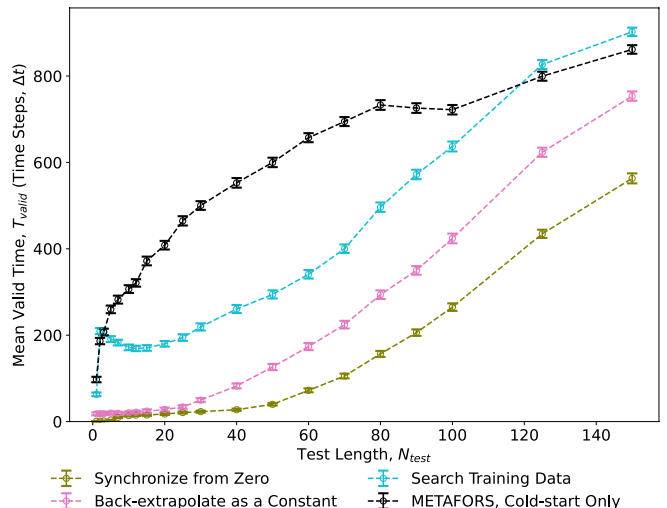


FIG. 8: **METAFORS is useful for cold-starting even when generalization is not required.** Using a library comprising $N_L = 1$ long time series, this single training signal and all 625 test signals are segments of the attractor for the standard Lorenz system, $\omega_t = 1$ and $v_1 = 10$, with different initial conditions. Since there is only one library member, the signal mapper learns only a cold-start vector, $\mathbf{r}(0)$, for the forecaster. For all methods, we train the forecaster parameters on the library signal directly. The training and test signals are partially-observed, containing only the x_3 Lorenz variable. Error bars denote the standard error of the mean.

larization. In Fig. 13, we show that in this case, with data from dynamical systems governed by the Lorenz-63 equations, our RC implementation of *METAFORS* benefits from using a high regularization strength (10^{-6}) for the linear regression step of the forecaster RC's training. When training a forecaster RC optimally for prediction of test systems with identical dynamics to the training system, a lower regularization strength (10^{-13}) provides better performance. This low regularization strength allows for an excellent fit to the training dynamics, and for higher valid prediction times than are achievable when generalization is required (Fig. 7). When generalization to new dynamics is our goal, a higher regularization prevents over-fitting to the training system but limits peak performance.

In both the partially-observed (Figs. 7 and 8) and fully-observed (Fig. 12) cases, *METAFORS* offers useful forecasts with test signals consisting of only one data point (the point in phase space from which the forecast should start). While cold-starting from such a short test signal is noteworthy, these library and test signals contain no observational noise. In Fig. 14, we demonstrate that our RC implementation of *METAFORS* is robust to small amounts of observational noise in the test signals.

III. DISCUSSION

This work introduces Meta-learning for Tailored Forecasting from Related Time Series (METAFORS), a framework designed to address significant challenges in forecasting dynamical systems from limited observations. By leveraging a library of machine learning models trained on related systems (for which extensive data are available), METAFORS demonstrates the ability to construct and initialize forecasting models tailored to test systems with limited observations, without requiring any explicit knowledge of the test or training systems’ underlying dynamics. Our study demonstrates the capabilities of METAFORS in multiple nonlinear systems, demonstrating its robustness, versatility, and potential applicability to real-world systems.

METAFORS addresses two critical challenges commonly faced by memory-based machine learning (ML) forecasters: brittleness and the requirement for substantial system-specific training data. By constructing a “signal mapper” to utilize a library of individually trained ML models, METAFORS identifies suitable forecasting model parameters and cold-start vectors from short observation signals. The results presented here highlight METAFORS’ unique advantages:

1. **Generalization Across Systems:** METAFORS successfully forecasts the behavior of test systems with dynamics that are related to, yet substantially different from, those in the training library. It achieves this generalization without contextual awareness or knowledge of governing dynamical parameters, as evidenced by its ability to replicate the logistic map’s bifurcation diagram, simultaneously learn and generalize the logistic and Gauss iterated maps, and generalize to Lorenz dynamics generated with dynamical parameters that differ substantially from those used to construct the training data.
2. **Cold-Starting Forecasts:** The ability to cold-start memory-based models is crucial when test signals are very short. METAFORS consistently outperforms our baseline methods, even enabling useful forecasts with minimal initialization data. This capability is particularly important for systems where data collection is constrained, as is the case in many biomedical, epidemiological, and ecological applications.
3. **Flexibility in Model Architecture:** METAFORS is not tied to specific ML architectures or training schemes. In our examples, we use reservoir computing for both the forecaster and signal mapper, but the principles of METAFORS are general and can accommodate other ML implementations for the forecaster or signal mapper.
4. **Ability to Simultaneously Capture Short-term Evolution and Long-term Behavior:** METAFORS is able to simultaneously predict both short-term evolution and long-term statistics (climate) of dynamical systems, making it applicable to a wide range of forecasting scenarios.
5. **Accuracy and Efficiency when Implemented with Reservoir Computing:** While METAFORS is framework-agnostic, our implementation with reservoir computers (RCs) leverages their appealing features – simplicity, computational efficiency, and low data and initialization requirements – while also extending the utility of traditional reservoir computing to tackle more challenging forecasting problems that require generalization.

Previous work has demonstrated that memory-based ML models with input channels for explicit context-indicators can capture the climate of unseen systems whose behaviors are qualitatively different but whose dynamics are governed by equations of the same functional form^{26–30}. By contrast, METAFORS achieves this generalization with no such contextual awareness. Instead, METAFORS’ signal mapper learns the context directly from short cue signals and then both constructs and initializes a tailored forecasting model. Since METAFORS constructs models from observational data alone, it requires little domain-specific knowledge. In Section IID, we exploit this versatility and train METAFORS to learn, simultaneously and without context, dynamical systems that are governed by two distinct functional forms (logistic and Gauss iterated maps). Parameter-aware generalization schemes cannot readily be extended to this setting without adding additional contextual indicators about the type of system from which training and test signals are drawn.

While METAFORS’ data-driven modeling approach is an important strength, the integration of METAFORS with hybrid forecasting architectures—where knowledge-based models are coupled with data-driven components—could further enhance its utility. Exploring such integrations could enable METAFORS to address scenarios where partial knowledge of the system dynamics is available, combining the strengths of data-driven and knowledge-based approaches.

Although the framework of METAFORS is not tied to a specific ML architecture, it is noteworthy that the reservoir computing implementation of METAFORS we develop here not only inherits the simplicity, versatility, and computational efficiency of RCs generally (with training achieved by simple linear regression), but constitutes an important extension of reservoir computing itself. Yan et al.⁵³ recently identified generalizable reservoir computing as a key to facilitating industrial use of RCs. In tempering the requirements of identical training and test dynamics (‘brittleness’), lengthy training series (‘data-intensity’), and warm-up signals to initialize predictions, which all constrain RCs in applications beyond forecasting, METAFORS constitutes an important step towards this goal.

We are aware of a small number of related approaches to forecasting dynamical systems from limited data. Two recent papers have introduced methods to cold-start RCs²⁴ and LSTMs²⁵. However, these studies highlight the importance of cold-starting only in the context of short-term forecasting and do not address scenarios in which the test and training signals differ in both their dynamics and their initial conditions. Here, we show that a framework to generalize forecasting models more broadly across systems with

varied dynamics readily simplifies for this more limited purpose. Similarly, other meta-learning frameworks for dynamical systems are constrained to particular implementations or applications, either because they cannot cold-start forecasting models with memory or because they depend on specific ML architectures. Some, for instance, are formulated explicitly using convolutional neural networks to capture spatiotemporal dynamics³⁹ or rely on data-compressing ML architectures like autoencoders to perform the meta-learning task^{36,37,40}. METAFORS’ strength is its versatility: it both generalizes and cold-starts the forecasting model; it simultaneously predicts the test system’s short-term evolution and long-term climate; and it is flexible with respect to the architectures of both the forecaster and the signal mapper.

While METAFORS demonstrates significant promise, it also presents limitations that warrant further investigation. The current implementation requires uniformly sampled, sequential data for training and forecasting. Other implementations or extensions of METAFORS to handle irregularly sampled data or multiscale dynamics would broaden its applicability.

Finally, while we have demonstrated the utility of METAFORS in relatively simple nonlinear systems, its scalability to high-dimensional datasets and real-world applications remains an open question. Incorporating unsupervised learning techniques, such as autoencoders, to learn interpretable, low-dimensional representations of dynamics could improve METAFORS’ scalability and facilitate its application to more complex systems.

In conclusion, METAFORS represents a significant step forward in data-driven forecasting of dynamical systems. By leveraging meta-learning to tailor forecasting models from related systems to new test systems, METAFORS mitigates key limitations of traditional memory-based models, enabling accurate predictions from limited data. The framework’s flexibility, efficiency, and generalization capabilities provide a robust foundation for tackling pressing forecasting challenges, from modeling climate dynamics to advancing real-time predictive analytics in fields such as public health and neuroscience.

IV. METHODS

A. Forecasting with reservoir computers

This section provides background for the description of our reservoir computing implementation of METAFORS to be presented in Section IV B. The specific reservoir computing architecture that we employ is constructed after the one proposed by Jaeger and Haas in 2004⁵⁹. They referred to their version of a reservoir computer (RC) as an ‘echo state network’, but the two terms have become largely synonymous in many contexts. In their seminal work, Jaeger and Haas demonstrated the use of RCs in predicting and processing time series.

The central component of an RC is a recurrent neural network, the reservoir. Each of its nodes, indexed by i , has an

associated continuous-valued, time-dependent activation level $r_i(t)$. For a reservoir of size N_r nodes, we refer to the vector $\mathbf{r}(t) = [r_1(t), \dots, r_{N_r}(t)]^T$, containing the activations of all of its nodes, as the reservoir state at time t . It evolves in response to an input signal according to a dynamical equation with a fixed discrete time-step, Δt :

$$\begin{aligned} \mathbf{r}(t + \Delta t) = & (1 - \lambda)\mathbf{r}(t) \\ & + \lambda \tanh(A\mathbf{r}(t) + B\mathbf{u}(t) + C), \end{aligned} \quad (7)$$

where the $\tanh()$ function is applied element-wise, and the directed and weighted adjacency matrix A is an $N_r \times N_r$ matrix specifying the strength and sign of interactions between each pair of reservoir nodes. We say that the reservoir has memory if $\mathbf{r}(t + \Delta t)$ depends on the reservoir past history, $\mathbf{u}(t - m\Delta t)$ for $m > 0$, and (because, by Eq. (7), $\mathbf{r}(t)$ depends on $\mathbf{u}(t - \Delta t)$, $\mathbf{r}(t - \Delta t)$ depends on $\mathbf{u}(t - 2\Delta t)$, and so on) this will be the case if the right hand side of Eq. (7) explicitly depends on $\mathbf{r}(t)$ (i.e., if $(1 - \lambda)$ and/or the matrix A are nonzero). The N_{in} -dimensional input $\mathbf{u}(t)$ is coupled to the reservoir nodes at time t via an $N_r \times N_{in}$ input weight matrix B . C is an N_r -dimensional random vector of biases, which serves to break symmetries in the dynamics of the reservoir nodes. λ , the leakage rate, influences the time-scale on which the reservoir state evolves; when the leakage rate is zero, $\mathbf{r}(t + \Delta t) = \mathbf{r}(t) \forall t$ and the reservoir does not evolve; when the leakage rate is one, the first term in Eq. (7) is zero and the reservoir ‘forgets’ its previous states more rapidly.

We use the *rescompy* python package⁶⁰ to construct our RCs. The adjacency matrix, A , of each reservoir is a (sparse) random directed network with connection probability $\langle d \rangle / N_r$ for each pair of nodes, where $\langle d \rangle$ is the mean in-degree of the network. We assign non-zero elements of A random values from a uniform distribution $U[-1, 1]$. Then we normalize this randomly generated matrix such that its spectral radius (eigenvalue of largest absolute value) has some desired value, ρ . We generate a dense input matrix, B , and a bias vector, C , by choosing each entry from the uniform distributions $U[-\sigma, \sigma]$ and $U[-\psi, \psi]$, respectively. We refer to σ as the input strength and to ψ as the bias strength.

For each step $\mathbf{u}(t)$ of an input series, we can construct a corresponding reservoir output, $\mathbf{y}(t)$, of dimension N_{out} , as a linear combination of the node activations resulting from its input to the reservoir:

$$\mathbf{y}(t) = W_{out}\mathbf{r}(t + \Delta t). \quad (8)$$

W_{out} is the $N_{out} \times N_r$ matrix that determines the linear combination. We call W_{out} the reservoir’s output layer and refer to the combination of a reservoir (defined by its internal parameters: the adjacency matrix, A , input matrix, B , bias vector, C , and leakage rate, λ) and an output layer, W_{out} , as a reservoir computer (RC). When training an RC for forecasting tasks, we choose its output layer so that at every time-step over some training signal of N_{train} evenly-spaced data points, i.e. with duration $(N_{train} - 1)\Delta t$, the RC’s output closely matches its input at the next time-step:

$$\mathbf{u}(t + \Delta t) \approx \mathbf{y}(t) = W_{out}\mathbf{r}(t + \Delta t). \quad (9)$$

In this case, $N_{out} = N_{in} = N_{sys}$, where N_{sys} is the number of observables we wish to predict. The internal parameters of the reservoir are unaltered during training. To calculate the output layer, we drive the reservoir with the training signal in the open-loop mode (Eq. (7) and Fig. 2a) and minimize the ridge-regression cost function:

$$\sum_{n=N_{trans}+1}^{N_{train}} \frac{\|W_{out} \mathbf{r}(n\Delta t) - \mathbf{u}(n\Delta t)\|^2}{N_{fit}} + \alpha_F \|W_{out}\|^2, \quad (10)$$

where the scalar α_F is a (Tikhonov⁶¹) regularization parameter which prevents over-fitting, $\|\cdot\|$ denotes the Euclidean (L^2) norm, and $N_{fit} = N_{train} - N_{trans}$ is the number of input/output pairs used for fitting. We discard the first N_{trans} data points as a transient to allow the reservoir state to synchronize to the input signal before fitting over the remaining time steps. The minimization problem, Eq. (10), has solution

$$W_{out} = YR^T (RR^T + \alpha_F N_{fit} I)^{-1}, \quad (11)$$

where I is the identity matrix and Y ($N_{out} \times N_{fit}$) and R ($N_r \times N_{fit}$), with n^{th} columns $\mathbf{u}([N_{trans} + n]\Delta t)$ and $\mathbf{r}([N_{trans} + n]\Delta t)$, respectively, are the target and reservoir state trajectories over the fitting period.

Once we have trained a reservoir computer (RC) as above, we can use it to obtain predictions, $\hat{\mathbf{u}}(t)$, of $\mathbf{u}(t)$, for values of $t > t_0 \geq N_{train}\Delta t$, where t_0 is the forecast start time. In the prediction phase, the RC evolves autonomously in closed-loop mode (Fig. 2B) by setting its input at each time-step to be its output from the previous time-step in a cyclic manner. The RC itself thus forms an autonomous dynamical system which evolves according to the coupled equations

$$\begin{aligned} \mathbf{r}(t + \Delta t) = & (1 - \lambda)\mathbf{r}(t) \\ & + \lambda \tanh(A\mathbf{r}(t) + B\hat{\mathbf{u}}(t) + C) \end{aligned} \quad (12a)$$

$$\hat{\mathbf{u}}(t + \Delta t) = W_{out} \mathbf{r}(t + \Delta t) \quad (12b)$$

and mimics the system of interest.

It is worthwhile to consider the separate roles of the reservoir state, $\mathbf{r}(t)$, and output layer, W_{out} , in the autonomous RC system, Eq. (12). We give a brief outline of these roles here and point to the work of Lu, Hunt, and Ott²³ for a more complete explanation and for discussion of the conditions under which this description holds.

In general, the reservoir component of an RC that has been successfully trained to accomplish its time series prediction task satisfies the *echo state property*^{62–66}: if the reservoir is driven in the open-loop mode (Eq. (7) and Fig. 2a) twice with the same input signal but different initial reservoir states, it will converge in both cases to the same trajectory after sufficient time. In other words, after some transient response of the reservoir has passed, its state becomes independent of its initial condition and depends only on the history of the input. One consequence of the echo state property is that any input trajectory \mathbf{u} that evolves on some manifold, M_{sys} will drive the reservoir to evolve along a trajectory, \mathbf{r} , such that once the transient period has passed, \mathbf{r} and \mathbf{u} are synchronized and \mathbf{r}

lies on some corresponding manifold, M_{res} , in the reservoir state-space^{23,65,66}. The output layer of an RC trained on \mathbf{u} maps points on or near M_{res} to points on or near M_{sys} . For a fixed reservoir (defined by its internal parameters A , B , C , and λ), the structures of these manifolds and, consequently, of the RC's output layer are determined solely by the dynamics of the system from which \mathbf{u} is sampled – the initial conditions of the reservoir and of the time series \mathbf{u} have negligible impact if N_{trans} and N_{train} are sufficiently large. We may thus build the following intuition, which is central to our RC implementation of METAFORS: an output layer, W_{out} , of an RC encodes the dynamics of the system on the manifold M_{sys} ; the reservoir state, $\mathbf{r}(t)$, determines its phase.

Generally, we expect the error in an RC's forecast to grow with time. There are two sources of this error:

- (1) Initial State Error: If the reservoir state at the start of a prediction, $\mathbf{r}(t_0)$, is too far from the manifold M_{res} corresponding to the dynamics encoded by the RC's output layer, the forecast dynamics may be inconsistent with those of the output layer. If $\mathbf{r}(t_0)$ is close to M_{res} but is not well synchronized to the state of the true system at time $t = t_0$, the forecast will be out of phase with the true system.
- (2) Output Layer Error: Errors in the learned output layer, W_{out} , induce errors in the prediction $\hat{\mathbf{u}}(t) = W_{out} \mathbf{r}(t)$.

If the underlying system is chaotic, both types of errors are amplified as t increases.

Typically, to initialize a forecast, we drive the reservoir in the open-loop mode (Eq. (7) and Fig. 2a) with a sync signal, \mathbf{u}_{sync} , from the true system and then switch to the closed-loop mode (Eq. (12) and Fig. 2b) to forecast from the end of \mathbf{u}_{sync} . The sync signal can be significantly shorter than would be sufficient to train an RC accurately. Hence, an RC that has been trained on a long time series to accurately capture the dynamics of $\mathbf{u}(t)$, can be used to predict from a different initial condition by starting from a comparatively short sync signal. However, if the sync signal is too short, the initial state error (1) will lead to an inaccurate forecast even if the output layer can accurately capture the dynamics of the true system.

B. Our reservoir-computing implementation of METAFORS

Meta-learning for Tailored Forecasting from Related Time Series (METAFORS) leverages a library of long time series from related dynamical systems to build suitable forecasting models for similarly related test systems with limited available data. METAFORS uses two levels of learning to perform this task. Here, we use reservoir computing for both levels. In the first level, we train output layers for the 'forecaster reservoir' separately on each available signal to construct a library of corresponding forecaster RCs. In the second level, the 'signal mapper' RC, draws on all the dynamics represented in the library of forecaster RCs, and a short test signal from a system of interest, to both construct and initialize a suitable forecaster RC for that system. Our training scheme for

the signal mapper RC has elements in common with schemes used in RC-based similarity learning that have been applied to image recognition and classification^{67,68}. In our case, the signal mapper infers similarity between short observational time series and learns a mapping from these short series to corresponding output layers (trainable parameters) and initial reservoir states (cold-start vectors) for a forecaster RC.

Because of their simplicity, accuracy, and efficiency in both short-term forecasting and long-term climate replication, we believe RCs are a particularly strong choice for building the forecaster used in the first level of learning. For the signal mapper in the second level of learning, we chose RCs primarily for their convenience, but they remain a robust and effective option. Nonetheless, we anticipate that other types of ML approaches could also perform well for these functions and might have advantages in certain situations. Alternative methods might offer comparable or improved performance for the forecaster, additional flexibility or interpretability for the signal mapper, or even complementary benefits that enhance the overall framework's adaptability to different scenarios.

1. Requirements and scope

METAFORS requires that we have available a short observed test signal or cue, s_{test} , from the dynamical system we wish to predict as well as a collection, or library, $\{\mathbf{L}_i\}$, $i = 1, \dots, N_L$, of N_L long signals from systems that exhibit similar dynamics to the test system. In our RC implementation of METAFORS, the data from each time series must be sequential and sampled at even intervals, Δt , and must also be of the same dimension, which we denote N_{sys} . We emphasize that the library and test signals need not contain full information of the system state at each time step. N_{sys} is merely the number of observables we have data for and wish to predict. We do not require that all long signals have equal duration, but we assume that each is sufficiently long to train an RC well. METAFORS is most useful when the duration of the test signal, $t_{test} = (N_{test} - 1)\Delta t$, where N_{test} is the number of data points in the test signal, is insufficient to train an RC directly. METAFORS' ability to cold-start the forecaster RC is most useful when t_{test} is insufficient to synchronize its reservoir state to the test signal.

2. Constructing the library

We first learn an RC representation of each system in the set of long signals, using the same forecaster reservoir layer with $N_r = N_F$ nodes for each. We refer to any combination of the forecaster reservoir with a trained output layer, W_{out} , as a forecaster RC and construct a library of forecaster RCs as follows (Fig. 1A).

- (2a) Using the same reservoir layer for each of the available long series, $\mathbf{L}_i(t)$, we train a forecaster RC with training time series $\mathbf{u}(t) = \mathbf{L}_i(t)$ to obtain a set of corresponding output layers, $\{W_{out}^i\}$. The output layer W_{out}^i constitutes

the trainable parameters, θ_i , of the forecaster for library member i . We also store the reservoir trajectory, $\mathbf{r}_i(t)$, over the fitting period of each long signal.

- (2b) We divide each long signal into sub-signals consisting of N_{test} sequential data points. In this work, we extract all possible short signals of length N_{test} after discarding a transient of length N_{trans} , i.e.,

$$s_{ij}(k\Delta t) = \mathbf{L}_i(j\Delta t + k\Delta t) \quad \forall \begin{cases} 1 \leq i \leq N_L \\ j \geq N_{trans}, \\ 0 \leq k \leq N_{test} - 1 \end{cases} \quad (13)$$

where s_{ij} denotes the j^{th} sub-signal extracted from long signal \mathbf{L}_i and N_{trans} is the transient time, as in Eq. (10). Here j also indexes the time step at the start of the short signal, since we utilize the full set of possible short signals after the transient. Although we note that METAFORS can still perform strongly when short signals are subsampled from the long library signals.

- (2c) For each short signal, s_{ij} , we extract a corresponding initial reservoir state

$$\mathbf{r}_{ij}(0) = \mathbf{r}_i(j\Delta t) \quad (14)$$

from the stored reservoir trajectories, $\{\mathbf{r}_i\}$. $\mathbf{r}_{ij}(0)$ is a constructed cold-start vector, \mathbf{m}_{ij} , for the test signal s_{ij} (Fig. 1B).

Each library member in METAFORS comprises a long signal and its corresponding trained forecaster model. The set of short signals, associated initial reservoir states, and trained output layers $\{(s_{ij}, \mathbf{r}_{ij}(0), W_{out}^i)\}$ forms the training data for the signal mapper.

3. Training the signal mapper RC

We train the signal mapper RC, with $N_r = N_{SM}$ nodes in its reservoir, to map each short signal s_{ij} to the corresponding initial reservoir state and output layer pair, $(\mathbf{r}_{ij}(0), W_{out}^i)$, as follows (Fig. 1C).

- (3a) For each short signal, s_{ij} , in the library, we set the signal mapper to have initial reservoir state $\mathbf{r}^{SM}(0) = \mathbf{0}$. We then feed the short signal into the signal mapper and store the final state, $\mathbf{r}^{SM}(N_{test}\Delta t)$, of the resulting trajectory in the reservoir state-space.
- (3b) We use ridge regression to find a linear mapping, W_{SM} , from each such final reservoir state, $\mathbf{r}^{SM}(N_{test}\Delta t)$, to its corresponding pair $(\mathbf{r}_{ij}(0), W_{out}^i)$:

$$W_{SM} = PR^T (RR^T + \alpha_{SM} N_{short} I)^{-1}, \quad (15)$$

where N_{short} is the number of short signals in the library (the number of training pairs), and R ($N_{SM} \times N_{short}$) and P ($(N_{sys} + 1)N_F \times N_{short}$) are the horizontal concatenations of all final signal mapper states and all target pairs, $\mathbf{p}_{ij} = [\mathbf{r}_{ij}(0), W_{flat}^i]^T$, respectively. W_{flat}^i is a vector representation of the output-layer W_{out}^i with dimension $N_F N_{sys}$.

4. Making predictions

Given a test signal, s_{test} , we construct a tailored forecaster model to generate predictions (Fig. 1D).

- (4a) We feed the test signal into the signal mapper as in step (3a) and apply the mapping learned in step (3b) to extract an appropriate initial reservoir state (i.e., cold start vector), $r_{test}(0)$, and output layer, W_{out}^{test} (i.e., set of model parameters).
- (4b) We combine the inferred output layer, W_{out}^{test} , with the forecaster reservoir to construct a tailored forecaster RC for the test system. We then synchronize this RC to the test signal in open-loop mode (Fig. 2A) starting from the initial state $r(0) = r_{test}(0)$, and close the loop (Fig. 2B) after time $t_{test} = (N_{test} - 1)\Delta t$ to forecast from the end of the test signal. The reservoir inputs are then:

$$u(t) = \begin{cases} s_{test}(t), & 0 \leq t \leq t_{test} \\ \hat{u}(t), & t > t_{test} \end{cases}.$$

Thus, $\hat{u}(N_{test}\Delta t)$ is the first output of the forecaster RC to be fed back as its input. In other words, t_{test} corresponds to the forecast start time t_0 in Section IV A.

C. Testbeds for probing the utility of METAFORS

1. The logistic and Gauss iterated maps

For each long signal in the library, we simulate the logistic/Gauss iterated map for 2000 total iterations. We discard the first 1000 iterations of each to ensure that the time series used for training are well-converged to the system's attractor. Each signal's remaining $N_{train} = 1000$ points constitute a long library signal. We use the next $N_{trans} = 50$ iterations of each signal as a transient period to synchronize the internal state of the forecaster RC to the input series, and then fit the trainable parameters of the forecaster, contained in its output layer, to the remaining $N_{fit} = 950$ iterations. We forecast $N_{for} = 1000$ iterations beyond the end of each test signal. Since, in these experiments, we are interested only in the long-term statistics, or climate, of a forecast, we discard the first 500 of these predicted points before calculating cumulative probability distributions or plotting bifurcation diagrams.

As shown in Table I, the reservoir hyperparameters that we use for our experiments with the logistic map only (Section II C) and for our experiments with both the logistic and Gauss iterated maps (Section II D) are identical except for the input strengths, σ_F and σ_{SM} . We chose the size, mean in-degree, and bias of both networks to have values that typically allow for reasonably accurate forecasting with reservoir computers, and performed no experiment-specific tuning of these values. We chose the leakage rate and spectral radius of the signal mapper such that its memory is long. This long memory ensures that the final reservoir state of the signal mapper, after it has received a test signal as input, is influenced by many,

or all, of the data points in the test signal. We chose the input strength of both the forecaster and signal mapper networks such that the average of the product of the input weight matrix and the input data from the library is approximately one, $\langle Bu_i(t) \rangle_{i,t} = \langle BL_i(t) \rangle_{i,t} \approx 1$. We chose the remaining hyperparameters – the regularization strengths, forecaster leakage rate, and forecaster spectral radius – by coarse hand-tuning to allow for good, but not necessarily optimal performance. While more robust hyperparameter tuning may improve performance overall, our priority is to compare the relative performances of simple baseline methods on familiar systems, rather than to obtain highly optimized forecasts.

	Forecaster			Signal Mapper				
Reservoir Size	N_F	500			N_{SM}	1000		
Mean In-degree	$\langle d \rangle_F$	3			$\langle d \rangle_{SM}$	3		
Spectral Radius	ρ_F	0.2	0.2	0.9	ρ_{SM}	0.9		
Input Strength	σ_F	2.5	4.0	0.1	σ_{SM}	2.5	4.0	0.1
Bias Strength	ψ_F	0.5			ψ_{SM}	0.5		
Leakage Rate	λ_F	0.2	0.2	0.1	λ_{SM}	0.1		
Regularization	α_F	10^{-6}			α_{SM}	10^{-8}		

TABLE I: **Reservoir Hyperparameters**

For entries with multiple values, those values pertain, from left to right, to our experiments with the logistic map only (Section II C), the logistic and Gauss iterated maps (Section II D), and the Lorenz-63 equations (Section II E).

2. The Lorenz-63 equations

To generate the library and test signals, we integrate Eq. (6), using a fourth-order Runge-Kutta scheme with fixed time-step $\Delta t = 0.01$, with different values of v_1 and ω_t and starting from randomly chosen initial conditions. We hold the Lorenz parameters $v_2 = 28$ and $v_3 = 8/3$ fixed. To ensure that the full duration of each signal lies on its corresponding system's attractor and contains no transient behavior, we discard the first 1000 points of each generated trajectory. Except where otherwise indicated, the long library signals consist of $N_{train} = 6000$ sequential data-points. We use the $N_{trans} = 1000$ points of each signal as a transient to synchronize the internal state of the forecaster reservoir to the signal and fit the forecaster's output layer to the remaining $N_{fit} = 5000$ points. We choose the parameters v_1 and ω_t of the library members randomly from the uniform distributions $\omega_t \in U[0.75, 1.25]$ and $v_1 \in U[7.5, 12.5]$. We choose the test systems' parameters to form a rectangular grid spanning the region defined by $0.7 \leq \omega_t \leq 1.3$ and $7 \leq v_1 \leq 13$. The resolution of this grid is 30×30 in Fig. 6 and 25×25 for the other figures. We forecast $N_{for} = 3000$ data-points beyond the end of each test signal. The reservoir hyperparameters (Table I) for our experiments with the Lorenz-63 Equations were chosen as described for our experiments with the logistic map only and with both the logistic and Gauss iterated maps.

D. Baseline methods for comparison

Except in Section II E 3, we use the forecaster reservoir hyperparameters given in Table I for METAFORS and for all of the baseline methods included in our results. We also discard the same number of data points, N_{trans} , before fitting the forecaster RC's trainable parameters for all methods except *Training on the Test Signal*. Below we provide additional details for three baseline approaches that are not fully specified in the main text.

1. Training on the test signal

We train the forecaster reservoir separately on each short test signal. The reservoir has a zero-vector initial state, $\mathbf{r}(0) = \mathbf{0}$, at the start of each test signal and we discard the first N_{trans} data points before fitting. For our results with the logistic and Gauss iterated maps (Sections II C and II D),

$$N_{trans} = \begin{cases} 0 & N_{test} = 2 \\ \lfloor N_{test}/2 \rfloor & N_{test} < 10, \\ 5 & N_{test} \geq 10 \end{cases}$$

where $\lfloor \cdot \rfloor$ denotes floor division. For our results with the Lorenz-63 equations (Section II E),

$$N_{trans} = \begin{cases} \lfloor N_{test}/10 \rfloor & N_{test} < 100 \\ 10 & N_{test} \geq 100 \end{cases},$$

because we use a forecaster reservoir with a longer memory than in our results with the logistic and Gauss iterated maps. Training on the test signal directly is not possible if the test signal contains only a single data point ($N_{test} = 1$).

2. Multi-task learning

We train the forecaster reservoir on the union of all long library signals. We set the reservoir state to zero at the start of every library signal and discard the first N_{trans} data points of each before fitting the forecaster's output layer.

3. Interpolated/extrapolated forecaster

This method relies on knowledge of the dynamical parameters for each of the training and test systems. In our experiments with the logistic and Gauss iterated maps (Sections II C and II D), we implement this method as follows. If the dynamical parameter of the test system is within the range of the dynamical parameters of the library models, we perform element-wise linear interpolation between the model parameters of the nearest library member with dynamical parameter greater than that of the test system and the nearest library member with dynamical parameter less than that of the test system. If the test system's dynamical parameter is beyond

the range of the library members, we perform element-wise linear extrapolation using the nearest two library members.

In our experiments with the Lorenz-63 equations (Section II E), we rescale the parameters ω_i and v_1 associated with each of the library members such that they span a unit interval along both axes. If the dynamical parameters of the test system are within the convex hull of the library, we triangulate the test parameters with respect to those of the library members. Then we perform linear barycentric interpolation of the corresponding forecasters' trainable model parameters. If the test system is outside the convex hull of the library, we use the forecaster RC of the nearest library member.

ACKNOWLEDGMENTS

We thank Daniel Canaday for helpful conversations, insights, and suggestions. We also acknowledge the University of Maryland supercomputing resources (<http://hpcc.umd.edu>) made available for conducting the research reported in this paper. This work was supported in part by DARPA under contract W31P4Q-20-C-0077. D.N.'s contributions were also supported by the National Science Foundation Graduate Research Fellowship Program under Grant No. DGE 1840340. M.G.'s contributions were also supported by ONR Grant No. N000142212656. Any opinions, findings, and conclusions or recommendations expressed in this material are those of the authors and do not necessarily reflect the views of the National Science Foundation, the Department of Defense, or the U.S. Government.

V. REFERENCES

- ¹S. L. Brunton and J. N. Kutz, *Data-Driven Science and Engineering: Machine Learning, Dynamical Systems, and Control* (Cambridge University Press, 2019).
- ²T. Arcomano, I. Szunyogh, J. Pathak, A. Wikner, B. R. Hunt, and E. Ott, "A machine learning-based global atmospheric forecast model," *Geophysical Research Letters* **47**, e2020GL087776 (2020).
- ³S. Wein, A. Schüller, A. M. Tomé, W. M. Malloni, M. W. Greenlee, and E. W. Lang, "Forecasting brain activity based on models of spatiotemporal brain dynamics: A comparison of graph neural network architectures," *Network Neuroscience* **6**, 665–701 (2022).
- ⁴C. Pandarinath, D. J. O'Shea, J. Collins, R. Jozefowicz, S. D. Stavisky, J. C. Kao, E. M. Trautmann, M. T. Kaufman, S. I. Ryu, L. R. Hochberg, J. M. Henderson, K. V. Shenoy, L. F. Abbott, and D. Sussillo, "Inferring single-trial neural population dynamics using sequential auto-encoders," *Nature Methods* **15**, 805–815 (2018).
- ⁵E. L. Ray, L. C. Brooks, J. Bien, M. Biggerstaff, N. I. Bosse, J. Bracher, E. Y. Cramer, S. Funk, A. Gerding, M. A. Johansson, A. Rumack, Y. Wang, M. Zorn, R. J. Tibshirani, and N. G. Reich, "Comparing trained and untrained probabilistic ensemble forecasts of covid-19 cases and deaths in the united states," *International Journal of Forecasting* **39**, 1366–1383 (2023).
- ⁶O. B. Sezer, M. U. Gudelek, and A. M. Ozbayoglu, "Financial time series forecasting with deep learning : A systematic literature review: 2005–2019," *Applied Soft Computing* **90**, 106181 (2020).
- ⁷Z. Han, J. Zhao, H. Leung, K. F. Ma, and W. Wang, "A review of deep learning models for time series prediction," *IEEE Sensors Journal* **21**, 7833–7848 (2021).

- ⁸S. L. Brunton, J. L. Proctor, and J. N. Kutz, “Discovering governing equations from data by sparse identification of nonlinear dynamical systems,” *Proceedings of the National Academy of Sciences* **113**, 3932–3937 (2016).
- ⁹R. Wang, D. Maddix, C. Faloutsos, Y. Wang, and R. Yu, “Bridging physics-based and data-driven modeling for learning dynamical systems,” in *Proceedings of the 3rd Conference on Learning for Dynamics and Control*, Proceedings of Machine Learning Research, Vol. 144 (PMLR, 2021) pp. 385–398.
- ¹⁰N. Göring, F. Hess, M. Brenner, Z. Monfared, and D. Durstewitz, “Out-of-domain generalization in dynamical systems reconstruction,” (2024), arXiv:2402.18377 [cs.LG].
- ¹¹J. Pathak, A. Wikner, R. Fussell, S. Chandra, B. R. Hunt, M. Girvan, and E. Ott, “Hybrid forecasting of chaotic processes: Using machine learning in conjunction with a knowledge-based model,” *Chaos: An Interdisciplinary Journal of Nonlinear Science* **28**, 041101 (2018).
- ¹²Y. Zhang and Q. Yang, “A survey on multi-task learning,” *IEEE Transactions on Knowledge and Data Engineering* **34**, 5586–5609 (2022).
- ¹³Q. Yang, Y. Zhang, W. Dai, and S. J. Pan, *Transfer Learning* (Cambridge University Press, 2020).
- ¹⁴P. Brazdil, J. N. van Rijn, C. Soares, and J. Vanschoren, *Metalearning: Applications to Automated Machine Learning and Data Mining*, 2nd ed. (Springer, 2022).
- ¹⁵T. Hospedales, A. Antoniou, P. Micaelli, and A. Storkey, “Meta-learning in neural networks: A survey,” *IEEE Transactions on Pattern Analysis & Machine Intelligence* **44**, 5149–5169 (2022).
- ¹⁶C. Lemke, M. Budka, and B. Gabrys, “Metalearning: A survey of trends and technologies,” *Artif. Intell. Rev.* **44**, 117–130 (2015).
- ¹⁷S. J. Pan and Q. Yang, “A survey on transfer learning,” *IEEE Transactions on Knowledge and Data Engineering* **22**, 1345–1359 (2010).
- ¹⁸M. Feurer, J. Springenberg, and F. Hutter, “Initializing bayesian hyperparameter optimization via meta-learning,” *Proceedings of the AAAI Conference on Artificial Intelligence* **29** (2015), 10.1609/aaai.v29i1.9354.
- ¹⁹C. Lemke and B. Gabrys, “Meta-learning for time series forecasting and forecast combination,” *Neurocomputing* **73**, 2006–2016 (2010), subspace Learning / Selected papers from the European Symposium on Time Series Prediction.
- ²⁰T. S. Talagala, R. J. Hyndman, and G. Athanasopoulos, “Meta-learning how to forecast time series,” *Journal of Forecasting* **42**, 1476–1501 (2023).
- ²¹D. J. Gauthier, E. Bollt, A. Griffith, and W. A. S. Barbosa, “Next generation reservoir computing,” *Nature Communications* **12** (2021), 10.1038/s41467-021-25801-2.
- ²²Y. Zhang and S. P. Cornelius, “Catch-22s of reservoir computing,” *Phys. Rev. Res.* **5**, 033213 (2023).
- ²³Z. Lu, B. R. Hunt, and E. Ott, “Attractor reconstruction by machine learning,” *Chaos: An Interdisciplinary Journal of Nonlinear Science* **28**, 061104 (2018).
- ²⁴L. Grigoryeva, B. Hamzi, F. P. Kemeth, Y. Kevrekidis, G. Manjunath, J.-P. Ortega, and M. J. Steynberg, “Data-driven cold starting of good reservoirs,” (2024), arXiv:2403.10325 [math.DS].
- ²⁵F. P. Kemeth, T. Bertalan, N. Evangelou, T. Cui, S. Malani, and I. G. Kevrekidis, “Initializing LSTM internal states via manifold learning,” *Chaos: An Interdisciplinary Journal of Nonlinear Science* **31**, 093111 (2021).
- ²⁶D. Patel, D. Canaday, M. Girvan, A. Pomerance, and E. Ott, “Using machine learning to predict statistical properties of non-stationary dynamical processes: System climate, regime transitions, and the effect of stochasticity,” *Chaos: An Interdisciplinary Journal of Nonlinear Science* **31**, 033149 (2021).
- ²⁷L.-W. Kong, H.-W. Fan, C. Grebogi, and Y.-C. Lai, “Machine learning prediction of critical transition and system collapse,” *Phys. Rev. Res.* **3**, 013090 (2021).
- ²⁸D. Köglmayr and C. Răth, “Extrapolating tipping points and simulating non-stationary dynamics of complex systems using efficient machine learning,” *Scientific Reports* **14**, 507 (2024).
- ²⁹S. Panahi and Y.-C. Lai, “Adaptable reservoir computing: A paradigm for model-free data-driven prediction of critical transitions in nonlinear dynamical systems,” *Chaos: An Interdisciplinary Journal of Nonlinear Science* **34**, 051501 (2024).
- ³⁰L.-W. Kong, G. A. Brewer, and Y.-C. Lai, “Reservoir-computing based associative memory and itinerancy for complex dynamical attractors,” *Nature Communications* **15**, 4840 (2024).
- ³¹C. Finn, P. Abbeel, and S. Levine, “Model-agnostic meta-learning for fast adaptation of deep networks,” in *Proceedings of the 34th International Conference on Machine Learning*, Proceedings of Machine Learning Research, Vol. 70, edited by D. Precup and Y. W. Teh (PMLR, 2017) pp. 1126–1135.
- ³²H. Yao, Y. Wei, J. Huang, and Z. Li, “Hierarchically structured meta-learning,” (2019), arXiv:1905.05301 [cs.LG].
- ³³A. Raghu, M. Raghu, S. Bengio, and O. Vinyals, “Rapid learning or feature reuse? towards understanding the effectiveness of maml,” in *International Conference on Learning Representations* (2020).
- ³⁴A. A. Rusu, D. Rao, J. Sygnowski, O. Vinyals, R. Pascanu, S. Osindero, and R. Hadsell, “Meta-learning with latent embedding optimization,” in *International Conference on Learning Representations* (2019).
- ³⁵T. Wu, J. Peurifoy, I. L. Chuang, and M. Tegmark, “Meta-learning autoencoders for few-shot prediction,” (2018), arXiv:1807.09912 [cs.LG].
- ³⁶D. Canaday, A. Pomerance, and M. Girvan, “A meta-learning approach to reservoir computing: Time series prediction with limited data,” (2021).
- ³⁷M. Kirchmeyer, Y. Yin, J. Dona, N. Baskiotis, A. Rakotomamonjy, and P. Gallinari, “Generalizing to new physical systems via context-informed dynamics model,” in *Proceedings of the 39th International Conference on Machine Learning*, Proceedings of Machine Learning Research, Vol. 162, edited by K. Chaudhuri, S. Jegelka, L. Song, C. Szepesvari, G. Niu, and S. Sabato (PMLR, 2022) pp. 11283–11301.
- ³⁸Y. Yin, I. Ayed, E. de Bézenac, N. Baskiotis, and P. Gallinari, “Leads: Learning dynamical systems that generalize across environments,” in *Advances in Neural Information Processing Systems*, Vol. 34, edited by M. Ranzato, A. Beygelzimer, Y. Dauphin, P. Liang, and J. W. Vaughan (Curran Associates, Inc., 2021) pp. 7561–7573.
- ³⁹R. Wang, R. Walters, and R. Yu, “Meta-learning dynamics forecasting using task inference,” (2022), arXiv:2102.10271 [cs.LG].
- ⁴⁰S. Panahi, L.-W. Kong, B. Glaz, M. Haile, and Y.-C. Lai, “Unsupervised learning for anticipating critical transitions,” (2025), arXiv:2501.01579 [nlin.CD].
- ⁴¹Z. Lu and D. S. Bassett, “Invertible generalized synchronization: A putative mechanism for implicit learning in neural systems,” *Chaos: An Interdisciplinary Journal of Nonlinear Science* **30**, 063133 (2020).
- ⁴²J. Z. Kim, Z. Lu, E. Nozari, G. J. Pappas, and D. S. Bassett, “Teaching recurrent neural networks to modify chaotic memories by example,” (2020), arXiv:2005.01186 [cond-mat.dis-nn].
- ⁴³B. Schrauwen, D. Verstraeten, and J. Campenhout, “An overview of reservoir computing: Theory, applications and implementations,” (2007) pp. 471–482.
- ⁴⁴C. Sun, M. Song, D. Cai, B. Zhang, S. Hong, and H. Li, “A systematic review of echo state networks from design to application,” *IEEE Transactions on Artificial Intelligence* **5**, 23–37 (2024).
- ⁴⁵M. Lukoševičius and H. Jaeger, “Reservoir computing approaches to recurrent neural network training,” *Computer Science Review* **3**, 127–149 (2009).
- ⁴⁶K. Srinivasan, N. Coble, J. Hamlin, T. Antonsen, E. Ott, and M. Girvan, “Parallel machine learning for forecasting the dynamics of complex networks,” *Phys. Rev. Lett.* **128**, 164101 (2022).
- ⁴⁷A. Wikner, J. Pathak, B. Hunt, M. Girvan, T. Arcomano, I. Szunyogh, A. Pomerance, and E. Ott, “Combining machine learning with knowledge-based modeling for scalable forecasting and subgrid-scale closure of large, complex, spatiotemporal systems,” *Chaos: An Interdisciplinary Journal of Nonlinear Science* **30**, 053111 (2020).
- ⁴⁸G. Tanaka, T. Yamane, J. B. Héroux, R. Nakane, N. Kanazawa, S. Takeda, H. Numata, D. Nakano, and A. Hirose, “Recent advances in physical reservoir computing: A review,” *Neural Networks* **115**, 100–123 (2019).
- ⁴⁹Z. Lu, J. Pathak, B. Hunt, M. Girvan, R. Brockett, and E. Ott, “Reservoir observers: Model-free inference of unmeasured variables in chaotic systems,” *Chaos: An Interdisciplinary Journal of Nonlinear Science* **27**, 041102 (2017).
- ⁵⁰S. Krishnagopal, M. Girvan, E. Ott, and B. R. Hunt, “Separation of chaotic signals by reservoir computing,” *Chaos: An Interdisciplinary Journal of Nonlinear Science* **30**, 023123 (2020).
- ⁵¹J. Pathak, B. Hunt, M. Girvan, Z. Lu, and E. Ott, “Model-free prediction of large spatiotemporally chaotic systems from data: A reservoir computing approach,” *Phys. Rev. Lett.* **120**, 024102 (2018).
- ⁵²E. Bollt, “On explaining the surprising success of reservoir computing fore-

- caster of chaos? the universal machine learning dynamical system with contrast to var and dmd,” *Chaos: An Interdisciplinary Journal of Nonlinear Science* **31**, 013108 (2021).
- ⁵³M. Yan, C. Huang, P. Bienstman, P. Tino, W. Lin, and J. Sun, “Emerging opportunities and challenges for the future of reservoir computing,” *Nature Communications* **15**, 2056 (2024).
- ⁵⁴E. N. Lorenz, “The problem of deducing the climate from the governing equations,” *Tellus* **16**, 1–11 (1964).
- ⁵⁵R. C. Hilborn, *Chaos and Nonlinear Dynamics: An Introduction for Scientists and Engineers* (Oxford University Press, 2000).
- ⁵⁶E. N. Lorenz, “Deterministic nonperiodic flow,” *Journal of Atmospheric Sciences* **20**, 130 – 141 (1963).
- ⁵⁷A. Wikner, J. Harvey, M. Girvan, B. R. Hunt, A. Pomerance, T. Antonsen, and E. Ott, “Stabilizing machine learning prediction of dynamics: Noise and noise-inspired regularization,” (2022), arXiv:2211.05262 [cs.LG].
- ⁵⁸T. Tél and M. Gruiz, “Chaos in dissipative systems,” in *Chaotic Dynamics: An Introduction Based on Classical Mechanics* (Cambridge University Press, 2006) p. 113–190.
- ⁵⁹H. Jaeger and H. Haas, “Harnessing nonlinearity: Predicting chaotic systems and saving energy in wireless communication,” *Science* **304**, 78–80 (2004).
- ⁶⁰D. Canaday, D. Kalra, A. Wikner, D. A. Norton, B. Hunt, and A. Pomerance, “rescompy 1.0.0: Fundamental Methods for Reservoir Computing in Python,” GitHub (2024).
- ⁶¹A. N. Tikhonov, A. V. Goncharsky, V. V. Stepanov, and A. G. Yagola, “Regularization methods,” in *Numerical Methods for the Solution of Ill-Posed Problems* (Springer Netherlands, Dordrecht, 1995) pp. 7–63.
- ⁶²H. Jaeger, “The “echo state” approach to analysing and training recurrent neural networks,” GMD Report 148 (GMD - German National Research Institute for Computer Science, 2001).
- ⁶³M. Lukoševičius, “A practical guide to applying echo state networks,” in *Neural Networks: Tricks of the Trade: Second Edition*, edited by G. Montavon, G. B. Orr, and K.-R. Müller (Springer Berlin Heidelberg, Berlin, Heidelberg, 2012) pp. 659–686.
- ⁶⁴M. Cucchi, S. Abreu, G. Ciccone, D. Brunner, and H. Kleemann, “Hands-on reservoir computing: a tutorial for practical implementation,” *Neuromorphic Computing and Engineering* **2**, 032002 (2022).
- ⁶⁵J. A. Platt, A. Wong, R. Clark, S. G. Penny, and H. D. I. Abarbanel, “Robust forecasting using predictive generalized synchronization in reservoir computing,” *Chaos: An Interdisciplinary Journal of Nonlinear Science* **31**, 123118 (2021).
- ⁶⁶J. A. Platt, S. G. Penny, T. A. Smith, T.-C. Chen, and H. D. Abarbanel, “A systematic exploration of reservoir computing for forecasting complex spatiotemporal dynamics,” *Neural Networks* **153**, 530–552 (2022).
- ⁶⁷S. Krishnagopal, Y. Aloimonos, and M. Girvan, “Similarity learning and generalization with limited data: A reservoir computing approach,” *Complexity* **2018** (2018).
- ⁶⁸N. Schaetti, M. Salomon, and R. Couturier, “Echo state networks-based reservoir computing for mnist handwritten digits recognition,” in *International Conference on Computational Science and Engineering* (Paris, France, 2016).

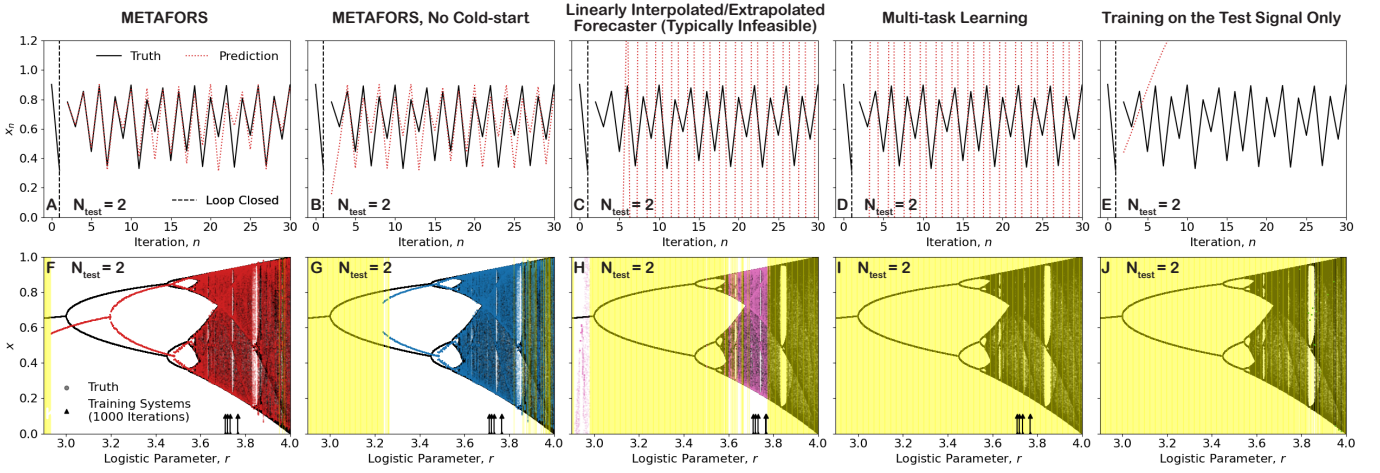


FIG. 9: In Section IIC, we demonstrate that METAFORS, when trained on just five stationary signals from the logistic map, can replicate the map’s dynamics across a large portion of its bifurcation diagram from test signals of just $N_{test} = 5$ data points with unknown dynamical parameters. We chose $N_{test} = 5$ so that the test signals would be long enough that our simple baseline comparison methods could succeed in some regions. Here, we demonstrate that METAFORS performs well even when the test signals contain just $N_{test} = 2$ data points. We train METAFORS on the same library of five trajectories from the logistic map with logistic parameters chosen randomly from $3.7 \leq r \leq 3.8$ (black arrows, **F to J**). All signals in the library are chaotic; periodic trajectories are excluded from selection. All test signals contain $N_{test} = 2$ iterations. (**A to E**) Example short-term forecasts obtained by METAFORS and baseline methods from a test signal with logistic parameters $r_1^* = 3.61$ and (**F to J**) bifurcation diagrams constructed by the same methods. Vertical yellow lines indicate values of r for which the corresponding forecast leaves the basin of attraction $0 \leq x \leq 1$ and does not return. In the true bifurcation diagram (**F to J**), we plot, for each of 500 evenly-spaced values of $2.9 \leq r \leq 4$, the final 500 iterations of a trajectory of total length 2000 iterations starting from a randomly chosen initial condition $0 < x_0 < 1$. We start each prediction at iteration 1000 of the corresponding true trajectory and discard the first 500 predicted iterations to ensure that the forecast long-term climate is not obscured on the plot by any initial transient behavior. We plot the subsequent 500 predicted iterations.

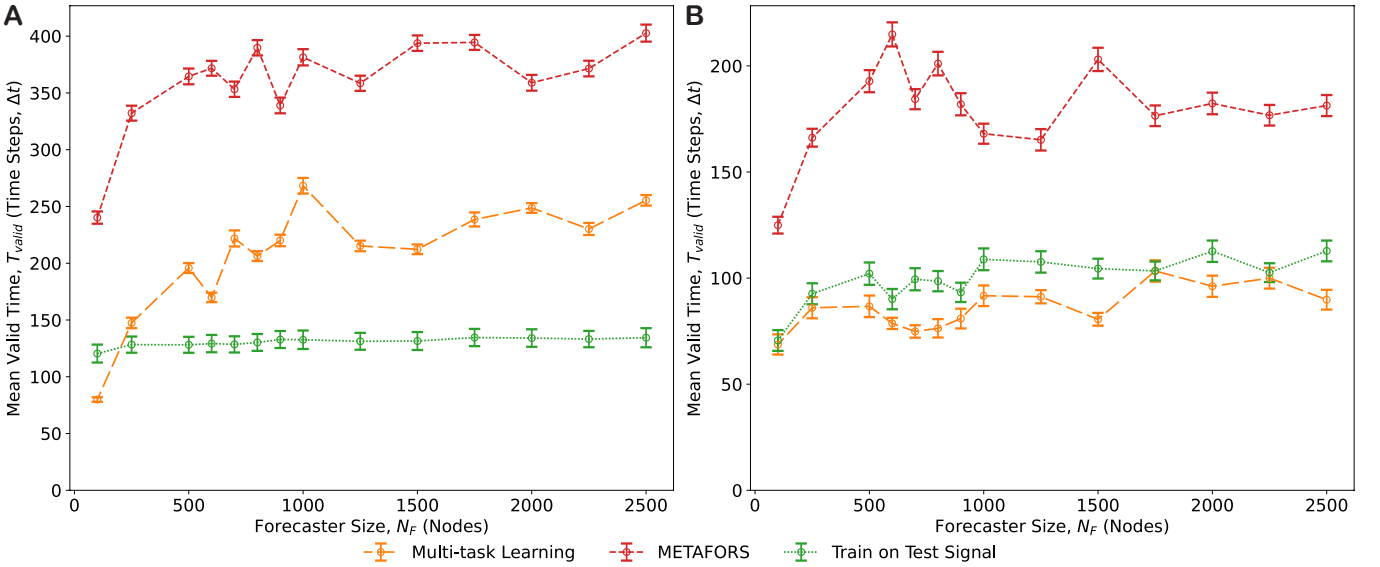


FIG. 10: Even with a more powerful forecaster (with more nodes), our simple multi-task learning approach cannot match METAFORS’ performance. We plot mean valid prediction time, T_{valid} , against forecaster size, N_F , with (**A**) fully-observed Lorenz systems and (**B**) partially-observed Lorenz systems (x_3 -only). In (**A and B**), the test signals have $N_{test} = 200$ sequential data points (long enough that METAFORS’ cold-starting of the forecaster offers no advantage over the other methods). The library consists of the same $N_L = 9$ long signals whose dynamical parameters are marked as black dots in Fig. 6 and we calculate mean valid times over a test set of 625 time series arranged in a 25×25 rectangular grid spanned by $7 \leq v_1 \leq 13$ and $0.7 \leq \omega_t \leq 1.3$, as in Section IV C 2. Error bars denote the standard error of the mean.

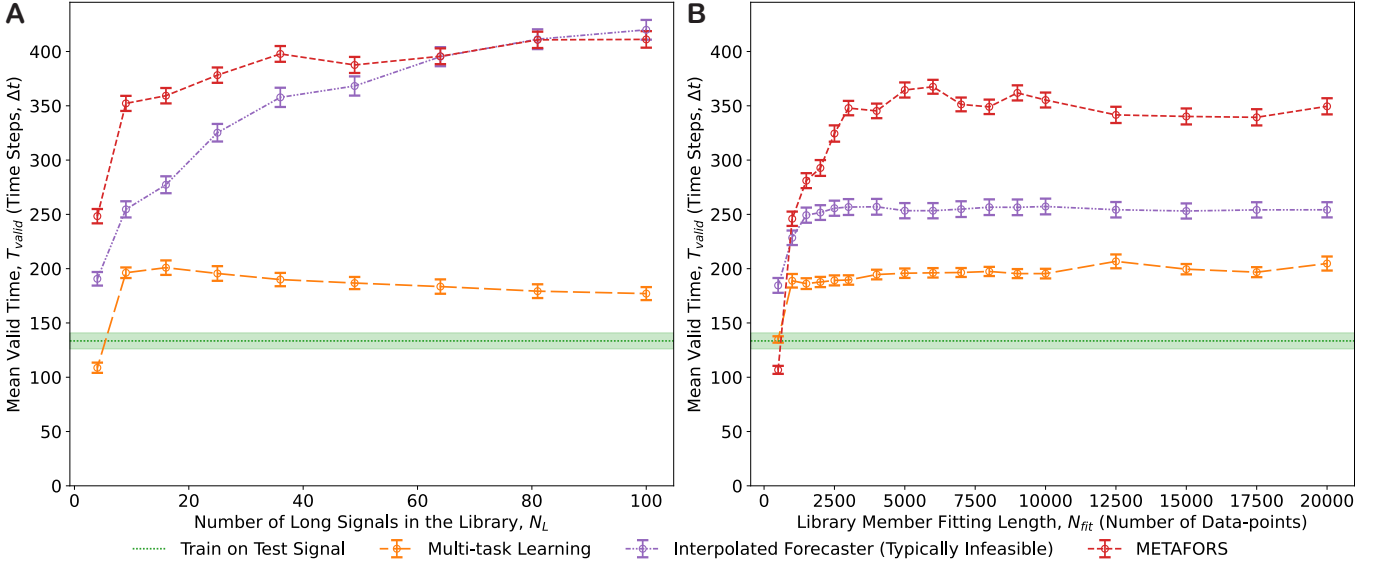


FIG. 11: In Fig. 6, we show how the performance of METAFORS and a few baseline forecasting methods depends on the relationship between the dynamical parameters of the test and library signals for a sample library containing $N_L = 9$ long signals of fixed length $N_{\text{train}} = 6000$ ($N_{\text{fit}} = 5000$). Here, explore how the structure of the library affects prediction quality on average over a range of range of dynamical parameters of the test signals. Namely, we plot mean valid prediction time against **(A)** the number of library members, N_L , and **(B)** the number of data-points in each long library signal used to fit the forecaster's trainable parameters, N_{fit} . In **(A)**, we fix $N_{\text{fit}} = 5000$. In **(B)**, we fix $N_L = 9$. In **(A and B)**, the test signals are of fixed length $N_{\text{test}} = 200$ and the library contains N_L long signals with Lorenz parameters chosen randomly from the uniform distributions $v_1 \in U[7.5, 12.5]$ and $\omega_t \in U[0.75, 1.25]$. We calculate mean valid times over a test set of 625 time series arranged in a 25×25 rectangular grid spanned by $7 \leq v_1 \leq 13$ and $0.7 \leq \omega_t \leq 1.3$, as in Section IV C 2. Error bars and shaded regions indicate the standard error of the mean. Independent of the fitting length, N_{fit} , we discard a transient of $N_{\text{trans}} = 1000$ data points at the start of each long library signal to train the forecaster RC. Note that the method *Linearly Interpolated/Extrapolated Forecaster* requires knowledge of the Lorenz parameters v_1 and ω_t governing the dynamics of the library and test signals.

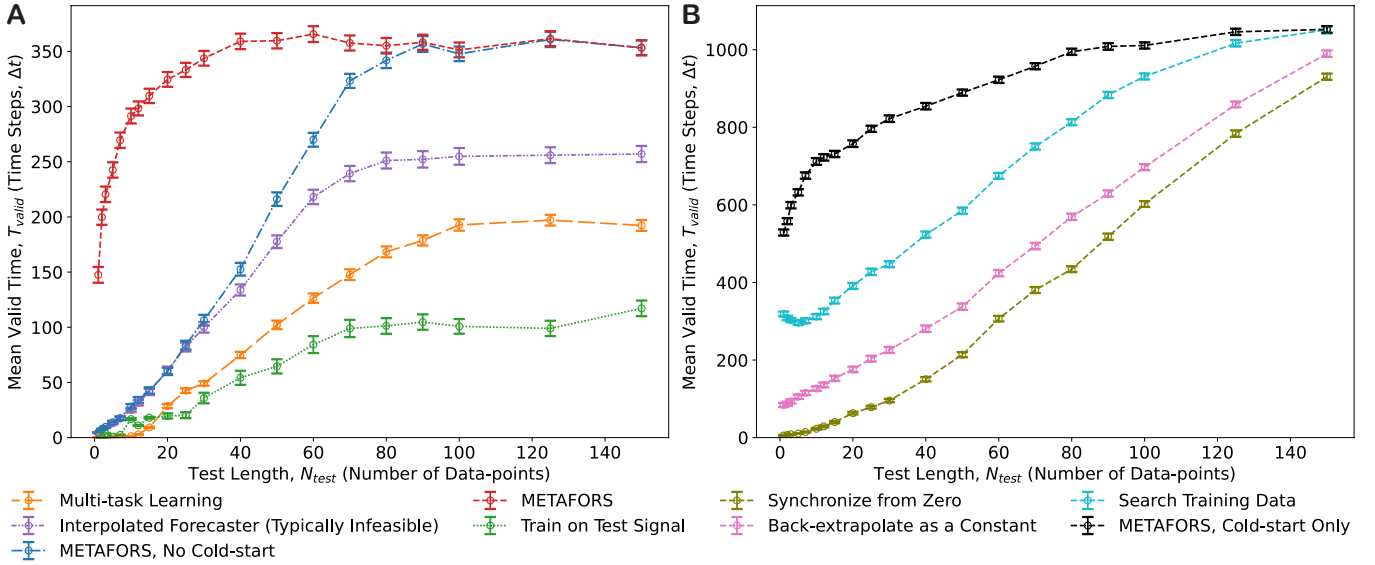


FIG. 12: We demonstrate in Figs. 7 and 8 that METAFOREs’ ability to cold-start the forecaster is essential when the test signals contain partial-state observations of Lorenz systems over very short durations. Here, we demonstrate the same result in the context of full-observed Lorenz systems. In (A), using a library comprising $N_L = 9$ long signals with Lorenz parameters indicated by the black dots in Fig. 6, we calculate mean valid times over 625 test signals arranged in a 25×25 rectangular grid spanning the space defined by $0.7 \leq \omega_t \leq 1.3$ and $7 \leq \nu_1 \leq 13$. For METAFOREs, No Cold-start (blue), the signal mapper RC learns model parameters but no cold-start vector for the forecaster. For that method and all others except METAFOREs, we synchronize the forecaster to the test signal from a zero-vector internal state, $r(0) = \mathbf{0}$, and then predict in autonomous/closed-loop mode (Fig. 2B) from the end of the test signal. In (B), we use a library comprising $N_L = 1$ long time series. This single training signal and all 625 test signals are segments of the attractor for the standard Lorenz system, $\omega_t = 1$ and $\nu_1 = 10$, with different initial conditions. Since there is only one library member, the signal mapper learns only a cold-start vector, $r(0)$, for the forecaster. For all methods, we train the forecaster parameters on the library signal directly. In (A and B), the training and test signals contain fully-observed Lorenz states and error bars denote the standard error of the mean.

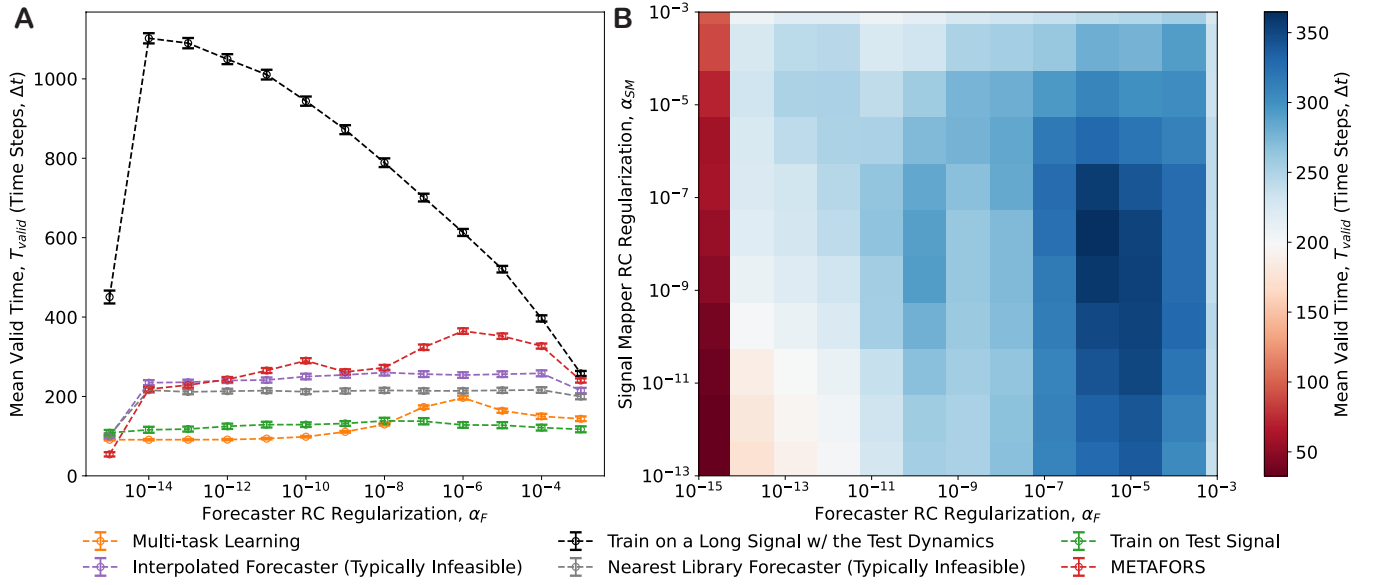


FIG. 13: In (A), we plot the mean valid time achieved by METAFORS and each of our baseline methods as we vary the regularization strength used to train the forecaster RC. In (B), we plot METAFORS' mean valid prediction time as both the forecaster regularization and the signal mapper regularization vary. In (A) and (B), we calculate mean valid times over a test set of 625 time series arranged in a 25×25 rectangular grid spanned by $7 \leq v_1 \leq 13$ and $0.7 \leq \omega_t \leq 1.3$, as in Section IV C 2. Error bars denote the standard error of the mean. The $N_L = 9$ long library signals consist of fully-observed Lorenz signals with Lorenz parameters depicted as black dots in Fig. 6. The test signals, of $N_{test} = 200$ sequential observations, are long enough to synchronize the forecaster's reservoir state well such that its initialization does not matter. The line labeled *METAFORS* in plot (A) is a horizontal slice along the line $\alpha_{SM} = 10^{-8}$ of the heatmap in plot (B). With our reservoir computing implementation of METAFORS (and our chosen reservoir hyperparameters, Table I), METAFORS' generalization benefits from a higher regularization than forecasting fixed dynamics. When training a forecaster RC optimally for prediction of test systems with identical dynamics to the training system, a lower regularization strength ($\alpha_F^{Trad} \approx 10^{-13}$) allows for an excellent fit to the training dynamics, and for high valid prediction times. When generalization to new dynamics is our goal, a higher regularization ($\alpha_F^{META} \approx 10^{-6}$) prevents overfitting to the training systems but limits peak performance. In general, there is likely a trade-off to consider when choosing the forecaster's regularization strength: if the regularization is too high, the library models will not represent well the dynamics of their corresponding training systems and the forecaster's performance will degrade; if the regularization is too low, the trainable parameters of the library models will not vary as smoothly with the dynamical parameters of the library signals, and it will be harder for the signal mapper to 'interpolate' between them. In the case of our experiments with the Lorenz results, METAFORS benefits from a higher regularization strength.

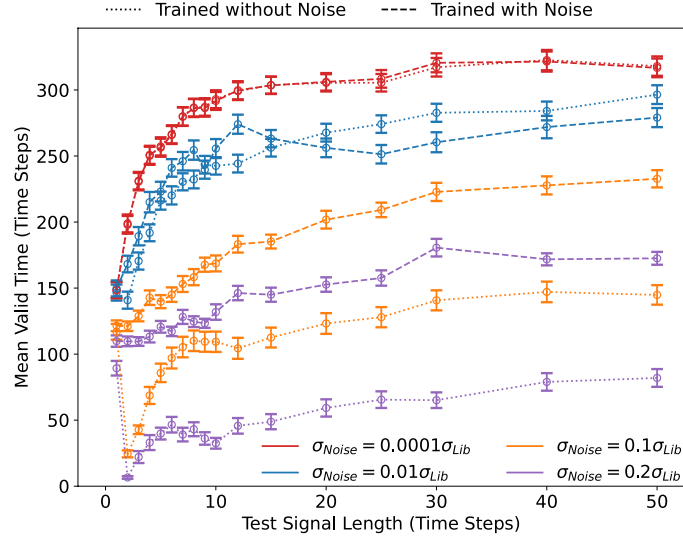


FIG. 14: METAFORS is robust to small amounts of noise. We plot METAFORS’ mean valid prediction time as a function of test signal length and noise-amplitude over 500 test signals. We add independent and identically distributed Gaussian observational noise with standard deviation, σ_{Noise} , in amplitude to each test signal before providing it to METAFORS. σ_{Noise} is expressed in multiples of the standard deviation in amplitude of all library members, σ_{Lib} , with both calculated component-wise. Dotted lines: we train METAFORS on ten noiseless, long fully-observed Lorenz signals selected randomly from the region spanned by $\omega_t \in [.8, 1.2]$ and $v_1 \in [8, 12]$. Dashed lines: we train METAFORS on the same long library signals, but with observational noise of equal amplitude to that of the test signals. In both cases, we measure valid prediction times against noiseless truth signals. Training on signals with noise of equal amplitude to that of the test signals represents the common scenario that the training and test data are both generated by the same process that is noisy or imperfectly measured. When the amplitude of noise in the test signals is low ($\sigma_{Noise} \lesssim 0.01\sigma_{Lib}$), METAFORS’ performance is strong independent of whether it has been trained on data that also contains noise. If the short test signals contain more significant noise ($\sigma_{Noise} \gtrsim 0.1\sigma_{Lib}$), METAFORS performance remains robust so long as it has been trained on data with similar levels of noise.